Supplementary Information for

A monodomain class II terpene cyclase assembles complex isoprenoid scaffolds

Philipp Moosmann[1,3†], Felix Ecker[2†], Stefan Leopold-Messer[1], Jackson K. B. Cahn[1], Cora L. Dieterich[1], Michael Groll[2], Jörn Piel[1]*

†These authors contributed equally to this work.
*Correspondence to: michael.groll@tum.de, jpiel@ethz.ch

This PDF file includes:

Table of contents

Supplementary Methods

Synthesis General Procedures Chemicals and solvents were purchased from commercial suppliers and were used without further purification. For silica gel chromatography, distilled technical grade solvents and silica gel SilicaFlash® P60 (Silicycle) were used. Thin layer chromatography (TLC) was performed using aluminum sheets "TLC Silica gel 60 F254" from Merck Millipore® and analysed with UV-light or by permanganate staining. LC-ESI mass spectrometry was performed on a Thermo Scientific Q Exactive mass spectrometer coupled to a Dionex Ultimate 3000 UPLC system. NMR spectra were recorded on a Bruker Avance III spectrometer equipped with a cold probe at 500 MHz for ^{1}H NMR and 125 MHz for ^{13}C NMR, as well as on a Bruker Avance III spectrometer equipped with a cold probe at 600 MHz for ^{1}H NMR and 150 MHz for ^{13}C NMR. Further a Bruker BBO 400MHz S1 and a Bruker BBO 500MHz S2 without a cold probe were used for the analysis of the synthetic intermediates. Chemical shifts are given in parts per million (ppm) and were referenced to the solvent peaks at δ_H 7.26 and δ_C 77.16 for $CDCl_3$. Multiplicities are given as follows: s - singlet, d - doublet, t - triplet, q - quartet, quint. - quintet, m - multiplet. The obtained data were processed and analysed with Bruker Topspin 3.5 software. UV/Vis spectra were measured at room temperature on the UV-Vis Spectrometer Cary 50 from Agilent Technologies. IR spectra were measured at room temperature on the Spectrum Two™ FT-IR Spectrometer from Perkin Elmer.
For the synthesis of **8** the procedure described by Lang M. and Steglich W. (2005) was followed[42].

Synthesis of (*E*, *E*)-farnesyl bromide (10)

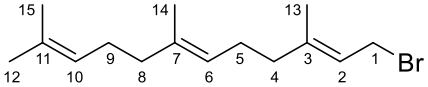

Farnesol (500 mg, 2.25 mmol, 1 eq., Sigma Aldrich) and PPh_3 (895 mg, 2.70 mmol, 1.2 eq.) were dissolved in 4 ml anhydrous CH_2Cl_2 and cooled to 0 °C. After addition of CBr_4 (649 mg, 247 mmol, 1.1 eq.) the reaction was stirred for 3.5 h. After the solvent was removed under reduced pressure, 20 ml sat. aq. $NaHCO_3$ were added to the residue and the aqueous phase was extracted with Et_2O (3 x 20 ml). The combined organic layers were washed with H_2O and brine, dried (Na_2SO_4) and concentrated. 10 ml of *n*-hexane were added to the residue and the flask was stored at -25 °C overnight. The precipitate was removed by filtration. The filter cake was washed 3 times with cold *n*-hexane. After some *n*-hexane was the flask was stored at -25 °C overnight, and the procedure was repeated the next day. Compound **10** was obtained as a brown oil (650 mg, 2.28 mmol, 91 %) from the filtrate after the complete removal of *n*-hexane.
^{1}H NMR (300 MHz, $CDCl_3$): δ 1.60 (s, 6 H), 1.68 (s, 3 H), 1.73 (s, 3 H), 1.94-2.16 (m, 8 H), 4.03 (d, 2 H, ^{4}J = 8.53 Hz), 5.05-5.13 (m, 2 H), 5.53 (t, ^{4}J = 8.53 Hz, 1 H). (Supplementary Fig. 18)
HRMS (m/z): $[M+H]^+$ = 285.1219 (calcd. 285.1212)

Synthesis of 3,4-dihydroxy-5-iodobenzaldehyde

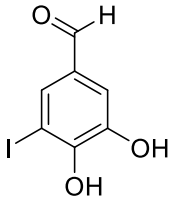

To a stirred solution of iodovanillin (1.39 g, 5.00 mmol, 1 eq.) a solution of BBr_3 (12.5 ml, 12.50 mmol, 2.5 eq., 1 M in CH_2Cl_2) was added at 0 °C under argon atmosphere. The reaction was stirred at room temperature for 4 h. Then the mixture was cooled to 0 °C and MeOH (2 ml/mmol) was added slowly. After refluxing for 40 min under argon atmosphere, the volatiles were evaporated and 30 ml H_2O were added and extracted with EtOAc (3 x 40 mL). The combined organic phases were washed with brine and dried over Na_2SO_4. The solvent was evaporated to yield the crude 3,4-dihydroxy-5-iodobenzaldehyde.

Synthesis of 3-iodo-4,5-bis(methoxymethoxy)benzaldehyde (11)

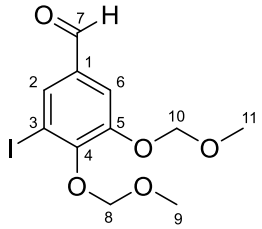

1.32 g of crude 3,4-dihydroxy-5-iodobenzaldehyde (5.00 mmol, 1 eq.) were suspended in 15 ml dry CH_2Cl_2. Under Argon atmosphere, MOM-Cl (2.5 ml, 15.00 mmol, 3 eq., 6 M in EtOAc) and *i*-Pr_2NEt (2.9 ml, 17.5 mmol, 3.5 eq.) were added. After stirring for 4.5 h at room temperature, the reaction was stopped by addition of 30 ml 2 N NH_4OH. The solution was extracted and extracted with Et_2O (3 x 40 ml) and the combined organic layers were washed with brine, followed by drying over Na_2SO_4. The solvent was removed under reduced pressure and **11** was obtained after purification by column chromatography (EtOAc:*n*-hexane = 2:5) as a colorless oil (1.363 g, 3.87 mmol, 77 % over two steps).

^{1}H NMR (400 MHz, $CDCl_3$): δ 3.49 (s, 3H, H-11), 3.65 (s, 3H, H-9), 5.24 (s, 2H, H-10), 5.31 (s, 2H, H-8), 7.62 (d, *J* = 1.86 Hz, 1H, H-6), 7.94 (d, *J* = 1.86 Hz, 1H, H-2), 9.81 (s, 1H, H-7). (Supplementary Fig. 19)

^{13}C NMR (400 MHz, $CDCl_3$): δ 56.7 (C-11), 58.7 (C-9), 92.7 (C-3), 95.2 (C-10), 99.1 (C-8), 116.3 (C-6), 134.0 (C-1), 135.2 (C-2), 149.9 (C-5), 151.7 (C-4), 189.6 (C-7). (Supplementary Fig. 20)

HRMS (m/z): $[M+H]^+$ = 352.9891 (calcd. 352.9880)

Synthesis of methyl 3-iodo-4,5-bis(methoxymethoxy)benzoate (12)

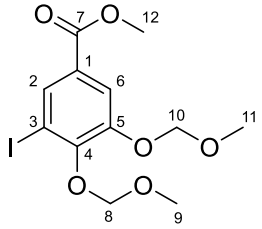

11 (1.00 g, 2.84 mmol, 1 eq.) was dissolved in 34 mL dry MeOH and cooled to 0 °C. A cold solution of KOH (414 mg, 7.38 mmol, 2.6 eq.) in 9.4 ml dry MeOH was added to the reaction, followed by the rapid addition of a cold solution of I_2 (934 mg, 3.69 mmol, 1.3 eq.) in 9.4 ml dry MeOH. The reaction was stirred for 15 min at 0 °C, then 40 mL of sat. aq. NH_4Cl and 16 mL sat. aq. $Na_2S_2O_3$ were added. The resulting mixture was extracted with EtOAc (3 x 100 mL) and the combined organic phases were washed with water and brine. The solution was dried over Na_2SO_4 and the solvent evaporated. After purification by column chromatography (EtOAc:*n*-hexane = 1:5) **12** was isolated as a yellow oil (1.022 g, 2.67 mmol) with a yield of 94%.

^{1}H NMR (400 MHz, $CDCl_3$): δ 3.52 (s, 3H, H-11), 3.68 (s, 3H, H-9), 3.91 (s, 3H, H-12), 5.25 (s, 2H, H-10), 5.29 (s, 2H, H-8), 7.79 (d, *J* = 1.93 Hz, 1H, H-6), 8.16 (d, *J* = 1.93 Hz, 1H, H-2). (Supplementary Fig. 21)

^{13}C NMR (400 MHz, $CDCl_3$): δ 52.5 (C-12), 56.7 (C-11), 58.6 (C-9), 92.1 (C-3), 95.3 (C-10), 99.5 (C-8), 117.8 (C-6), 127.7 (C-1), 134.1 (C-2), 149.1 (C-5), 150.5 (C-4), 165.3 (C-7). (Supplementary Fig. 22)

HRMS (m/z): $[M+H]^+$ = 382.9997 (calcd. 382.9986)

Synthesis of methyl 3,4-bis(methoxymethoxy)-5-((*2E,6E*)-3,7,11-trimethyldodeca-2,6,10-trien-1-yl)benzoate (13)

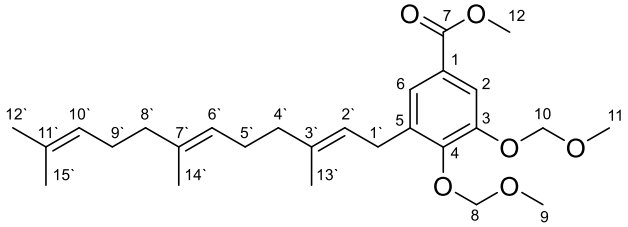

Compounds **10** and **12**, as well as all syringes used, were dried under high vacuum for 3 h prior to use. Compound **12** (250 mg, 0.654 mmol, 1.2 eq.) was dissolved in 3.3 mL dry, freshly degassed THF and cooled to -20 °C. 1.765 mL *i*-PrMgBr (130.1 mg, 0.883 mmol, 1.35 eq., 0.5 M in THF) were added dropwise at -20 °C and the reaction was stirred for 30 min at this temperature. 0.260 mL Li_2CuCl_4 (6 mg, 0.026 mmol, 0.04 eq., 0.1 M in THF) were added slowly and the reaction was stirred for 10 min at -20 °C before compound **10** (156 mg, 0.545 mmol, 1 eq.) in 1.7 mL dry, freshly degassed THF was added dropwise at -20 °C over a period of 45 minutes. The reaction was stirred for 1.5 h at -20 °C before 18 mL of sat. aq. NH_4Cl were added. The reaction mixture was extracted with Et_2O (3 x 75 mL) and the combined organic phases were washed with 4% aq. NH_4OH and brine before being dried over Na_2SO_4. The solvent was removed and compound **13** (110 mg, 0.239 mmol) was isolated with minor impurities as a clear oil with a yield of 37% after purification by column chromatography (EtOAc:*n*-hexane = 1:7). (Supplementary Fig. 23-28)

^{1}H NMR (400 MHz, $CDCl_3$): δ 1.59 (m, 6H, H-14`, H 15`), 1.67 (m, 3H, H-12`), 1.72 (m, 3H, H-13`), 1.93-2.17 (m, 8H, H-4`, H-5`, H-8`, H-9`), 3.44 (d, *J* = 7.16 Hz, 2H, H-1`), 3.51, 3.59 (s, 3H, H-9, H-11), 3.87 (s, 3H, H-12), 5.05-5.14 (m, 2H, H-6`, H-10`), 5.18, 5.23 (s, 2H, H-10, H-8), 5.31 (m, 1H, H-2`), 7.57 (d, *J* = 2.07 Hz, 1H, H-6), 7.65 (m, 1H, H-2). (Supplementary Fig. 23)

^{13}C NMR (400 MHz, $CDCl_3$): δ 16.1 (C-14`), 16.4 (C-13`), 17.8 (C-15`), 25.8 (C-12`), 26.7, 26.8 (C-9`, C-5`), 28.6 (C-1`), 39.8 (C-8`), 40.1 (C-4`), 52.2 (C-12), 56.5, 57.7 (C-9, C-11), 95.2, 99.1 (C-8, C-10), 115.2 (C-2), 122.1 (C-2`), 124.5, 124.6 (C-6`, C-10`), 125.0 (C-6), 125.9 (C-1), 131.4, 135.2 (C-7`, C-11`), 136.2 (C-5), 137.1 (C-3`), 149.0, 149.4 (C-3, C-4), 166.8 (C-7). (Supplementary Fig. 24)

HRMS (m/z): $[M+H]^+$ = 461.2896 (calcd. 461.2898)

Synthesis of 3,4-bis(methoxymethoxy)-5-((*2E,6E*)-3,7,11-trimethyldodeca-2,6,10-trien-1-yl)benzoic acid (14)

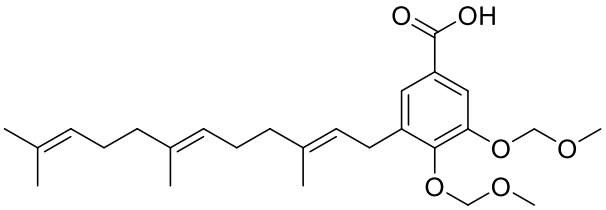

Compound **13** (49.0 mg, 106 µmol, 1 eq.) and LiOH · H_2O (8.9 mg, 212 µmol, 2 eq.) were suspended in 2.00 mL MeOH and 0.66 mL H_2O, refluxed for 3 h, before a second portion of LiOH · H_2O (6 mg, 143 µmol, 1.35 eq.) and 0.50 mL MeOH were added. The mixture was continued to reflux for 1.5 h and then quenched by addition of 20 mL H_2O. The aquatic phase was acidified with 1 N HCl and extracted with EtOAc (3 x 30 mL), the combined organic phases were washed with water twice before being dried over Na_2SO_4. The solvent was evaporated to give the crude acid **14** (42.0 mg) as a yellow oil.

Synthesis of 3-farnesyl-4,5-dihydroxybenzoic acid (8)

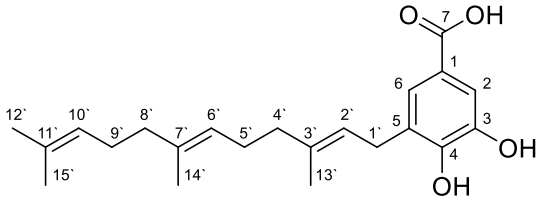

Crude **14** (40 mg, 89.6 µmol, 1 eq.) was dissolved in 1 mL dry *i*-PrOH and AcCl (20.5 µL, 286.7 µmol, 3.2 eq.) was added under argon atmosphere. The reaction was stirred for 5h at room temperature and poured on 20 mL H_2O. The aquatic phase was extracted with EtOAc (3 x 30 mL). The combined organic layers were washed with H_2O, dried (Na_2SO_4) and the solvent was evaporated. The product **8** (17 mg, 47.4 µmol) was obtained after column chromatography (MeOH:$CHCl_3$ = 1:9) as an off-white solid with a yield of 47% over two steps. (Supplementary Fig. 29-36)

IR (ATR, cm^{-1}): 3436, 3284, 3076, 2966, 2916, 2855, 1676, 1617, 1603, 1516, 1443, 1375, 1292, 1236, 1102, 987, 937, 890, 837, 777, 715, 562, 487.

^{1}H NMR (600 MHz, $CDCl_3$): δ 1.60 (m, 6H, H-14`, H 15`), 1.68 (m, 3H, H-12`), 1.79 (m, 3H, H-13`), 1.95-2.18 (m, 8H, H-4`, H-5`, H-8`, H-9`), 3.41 (d, *J* = 7.31 Hz, 2H, H-1`), 5.08 (m, 2H, H-6`, H-10`), 5.34 (m, 1H, H-2`), 7.50 (s, 2H, H-2, H-6). (Supplementary Fig. 29)

^{13}C NMR (600 MHz, $CDCl_3$): δ 16.0 (C-14`), 16.2 (C-13`), 17.6 (C-15`), 25.6 (C-12`), 26.1 (C-5`), 26.7 (C-9`), 29.8 (C-1`), 39.6 (C-8`), 39.8 (C-4`), 115.0 (C-2), 120.7 (C-2`), 121.1 (C-1), 123.4 (C-6`), 124.4 (C-10`), 124.8 (C-6), 127.1 (C-5), 131.4 (C-11`), 135.7 (C-7`), 139.5 (C-3`), 143.3 (C-3), 147.5 (C-4), 170.4 (C-7). (Supplementary Fig. 30)

HRMS (m/z): $[M-H]^-$ = 357.2083 (calcd. 357.2060) (Supplementary Fig. 35)

UV/Vis: λ_{max} 447 nm (Supplementary Fig. 36)

Structure elucidation of merosterolic acid B (9) Merosterolic acid B (**9**) had a molecular formula of $C_{27}H_{38}O_4$ as suggested by HR-LC-ESIMS (m/z 427.2837 $[M+H]^+$, Δ -0.596 mmu) suggesting nine instances of unsaturation (Supplementary Fig. 9). The ^{1}H NMR spectrum and the HSQC spectrum suggested the presence of four aliphatic singlet methyls, as well as one exomethylene (Supplementary Fig. 11 and 13). The chemical shifts of C-16 through C-22 were assigned to the dihydroxylated benzoate moiety (Supplementary Table 2). Five levels of unsaturation were localized to the benzoate moiety and an additional one to the exomethylene double bond. The lack of further alkene signals suggested the presence of three cycles. The COSY spectrum revealed four substructures, which were limited due to overlapping signals (Supplementary Fig. 10 and 12). HMBC correlations from H-17 and H-19 to C-22 connected the carboxylic acid to C-18 (Supplementary Fig. 14). Strong HMBC correlations from H-17 and H-19 to C-21 suggested the carbon's meta position to C-17 and C-19. HMBC correlations from H-17 to C-15 and H-15 to C16 and C-21 suggested that the aliphatic moiety is attached to C-16 of the benzoic acid. **Ring A** could be determined based on HMBC correlations from H-25 to C-1, C-5 and C-10, and from H-26 to C-3, C-4, C-5 and C-27. There were also strong correlations from H-27 to C-26. **Ring C** could be established with HMBC correlations from H-24 to C-8, C-9 and C-14, from H-14 to C-13, and from H-23 to C-12 and C-13. Further correlations from H-15 to C-13 and C-14, and from H-14 to C-15 connected ring C to the benzoic acid. HMBC correlations from H-25 to C-9 connected ring A with ring C. **Ring B** was completed with HMBC correlations from H-6 to C-7, and from H-7 to C-8 and C-24. Determination of the relative stereochemistry was attempted with NOESY and ROESY spectra (Supplementary Fig. 15 and 16), but remained ambiguous due to overlapping signals. NOEs between H-17 and H-14, H15 and H-23 support the proximity of ring C to the benzoic acid. NOEs between H-5 and H-9, as well as H-9 and H-14 suggested that the relative stereochemistry is the same as in merosterolic acid A (**2**), but unclear signals from H-24 through H-27 made a confirmation challenging.

Supplementary Figures and Tables

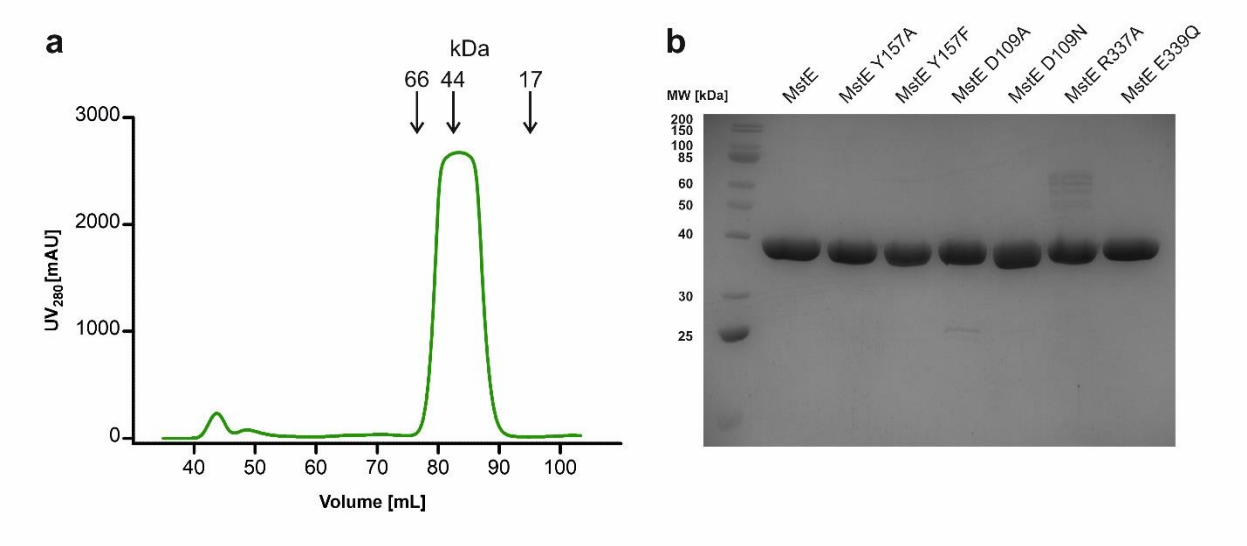

Supplementary Fig. 1. Purification of MstE.
(**A**) Size-exclusion chromatogram of MstE performed on a Superdex 200 16/60 column. Arrows mark retention volumes of reference proteins according to the manufacturer. (**B**) SDS-PAGE analysis of WT and mutant proteins applied in crystallographic experiments. Each lane contains 5 µg of protein.

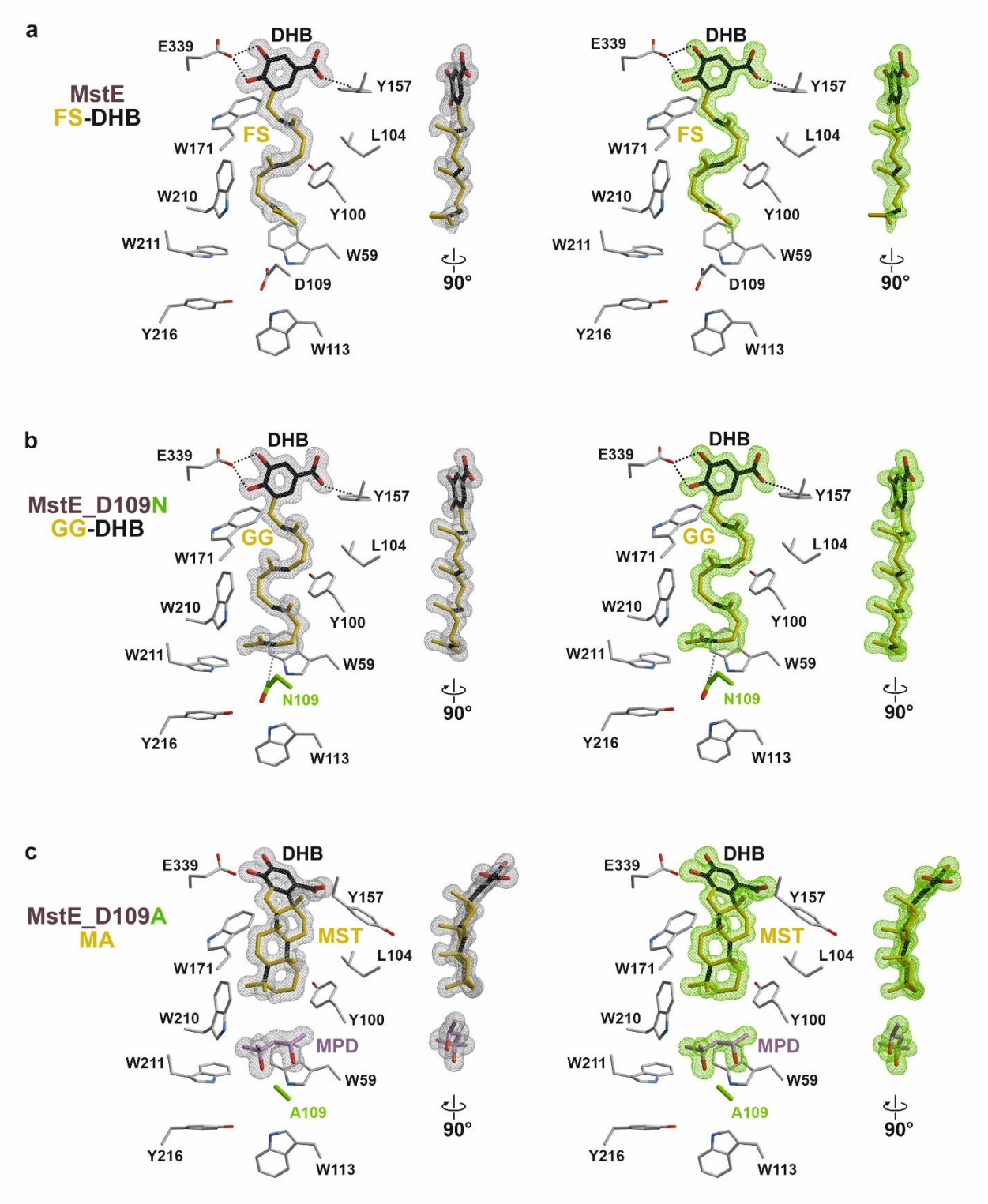

Supplementary Fig. 2. Electron density maps of ligands bound to MstE.
Left: Close-up views of the active sites in MstE:FS-DHB (**A**), MstE_D109N:GG-DHB (**B**) and MstE_D109A:MA (**C**). The $2F_O$-F_C electron density maps (gray mesh, contoured to 1.0 σ) of ligands are shown together with residues engaged in ligand binding. Side-views of ligands (rotated by 90°) are depicted

on the right. Right: The corresponding F_O-F_C electron density maps (green mesh, contoured to 3.0 σ) with ligands omitted for structure refinement.

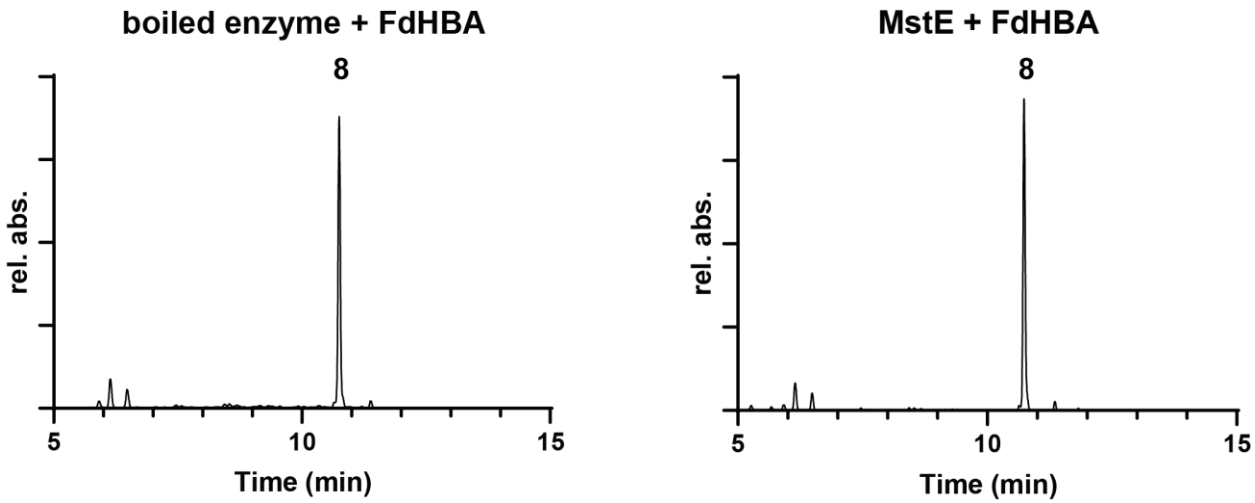

Supplementary Fig. 3. *In-vitro* activity of MstE with 3-farnesyl-4,5-dihydroxybenzoic acid (FdHBA) (8).
Shown are UV traces at 254 nm of HPLC chromatograms. The peak was assigned to 8 by mass spectrometry.

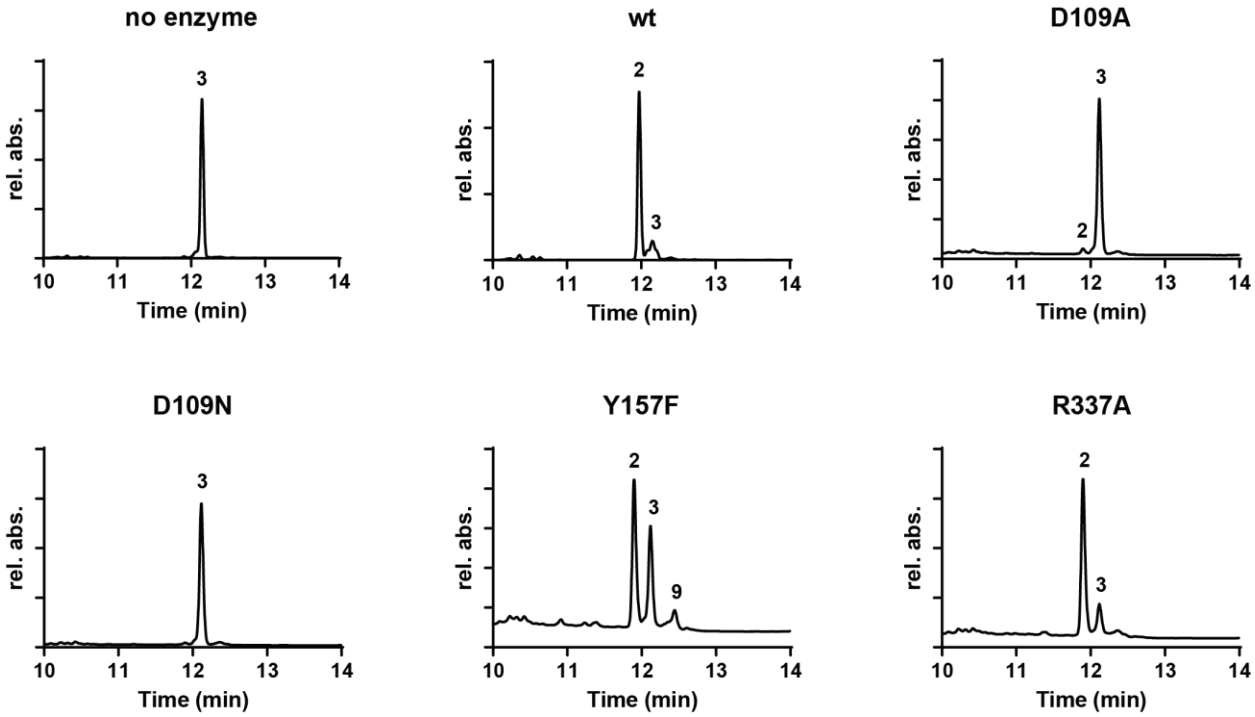

Supplementary Fig. 4. *In-vitro* activity of MstE single point mutants used for crystallographic studies. Shown are UV peaks (254 nm) of GG-DHB (3) and cyclized products merosterolic acid A (2) and merosterolic acid B (9). Peaks were identified based on their UV absorbance, *m/z*, and retention time.

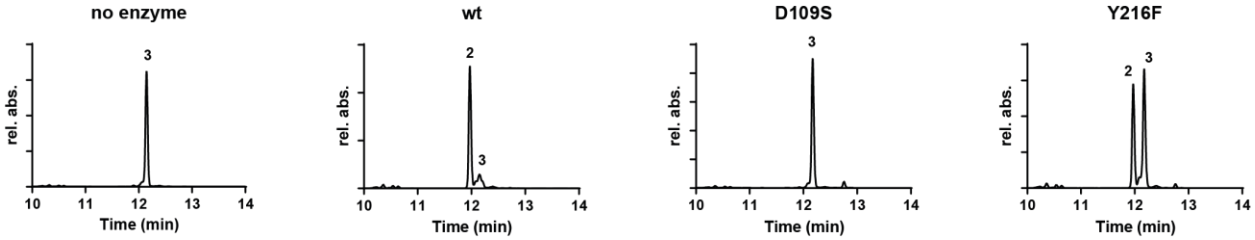

Supplementary Fig. 5. *In-vitro* activity of MstE single point mutants proposed to be involved in protonation.
Shown are UV peaks (254 nm) of GG-DHB (**3**) and cyclized product merosterolic acid A (**2**). Peaks were identified based on their UV absorbance, *m/z*, and retention time.

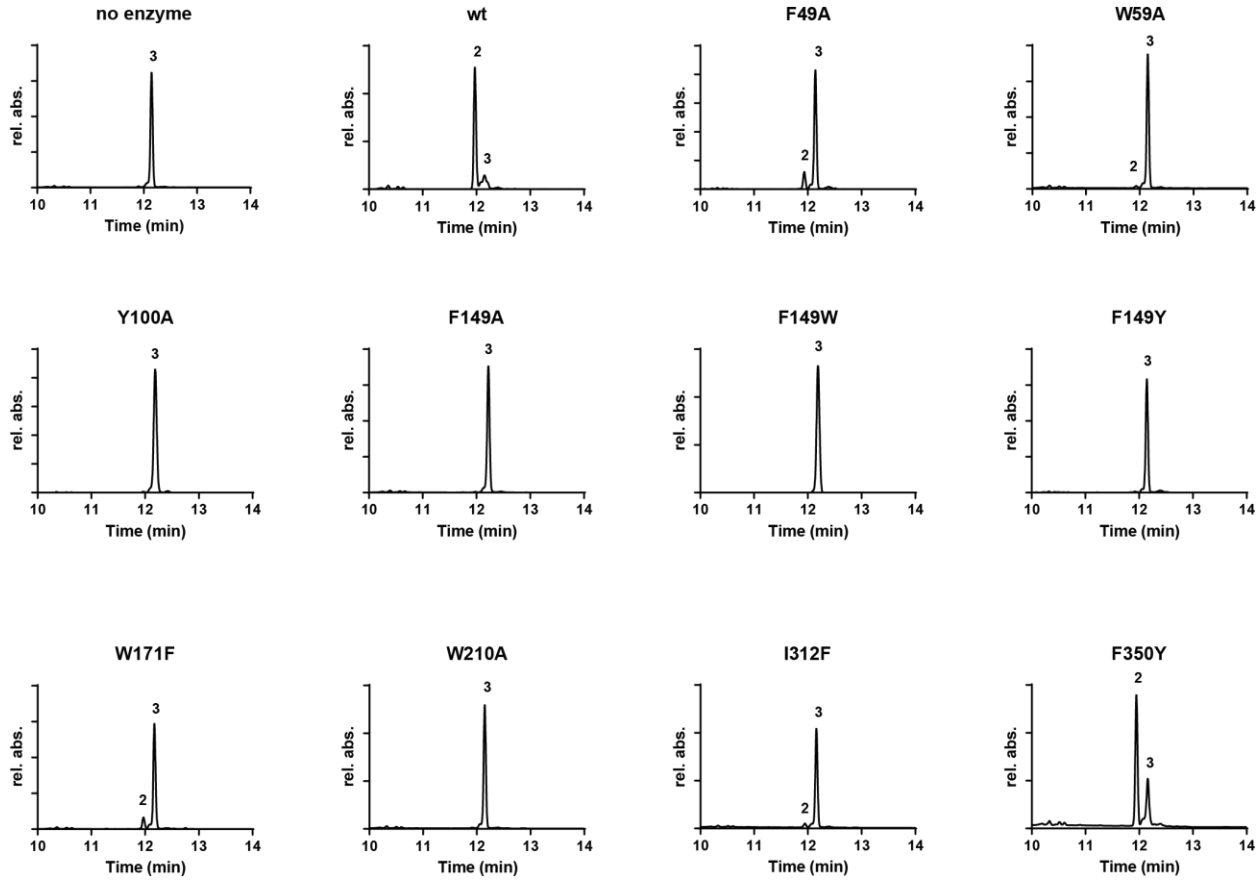

Supplementary Fig. 6. *In-vitro* activity of MstE single point mutants without relaxed activity. Shown are UV peaks (254 nm) of GG-DHB (**3**) and cyclized product merosterolic acid A (**2**) and. Peaks were identified based on their UV absorbance, *m/z*, and retention time. Aromatic residues F49, W59, Y100 and W210 show close interactions with the substrate in the crystal structures.

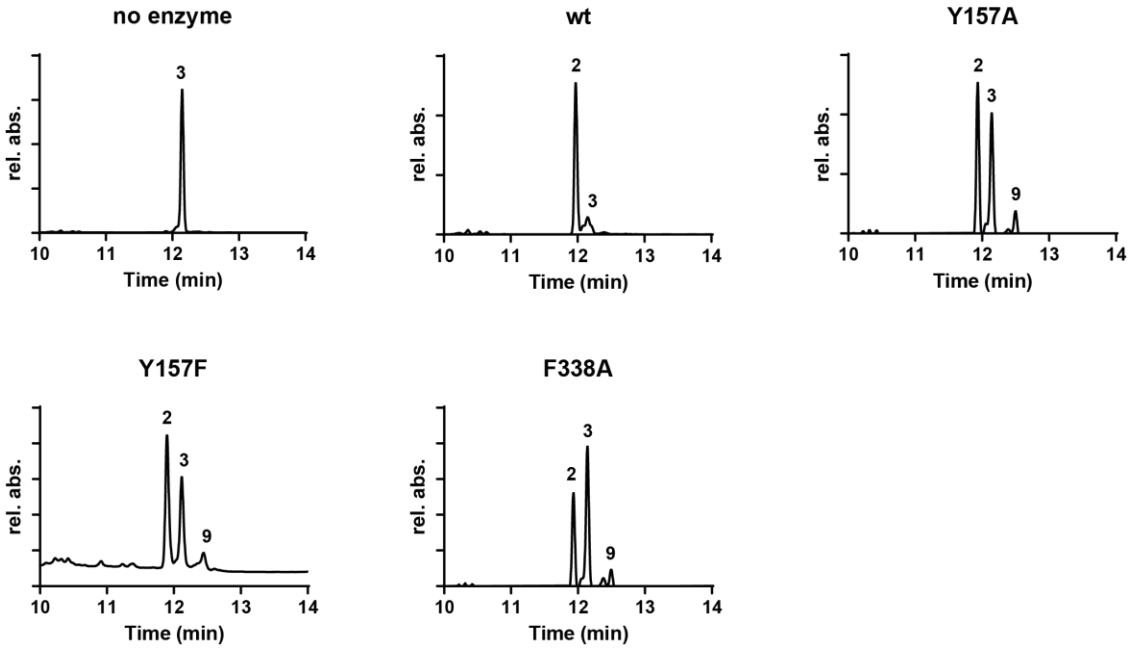

Supplementary Fig. 7. *In-vitro* activity of MstE single point mutants synthesizing new product merosterolic acid B.
Shown are UV peaks (254 nm) of GG-DHB (**3**) and cyclized products merosterolic acid A (**2**) and merosterolic acid B (**9**). Peaks were identified based on their UV absorbance, *m/z*, and retention time.

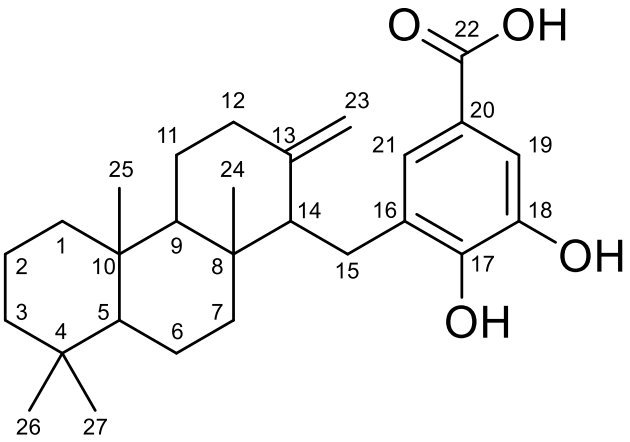

Supplementary Fig. 8. Structure of merosterolic acid B (9)
Carbon atoms are numbered for referencing the NMR data.

A)

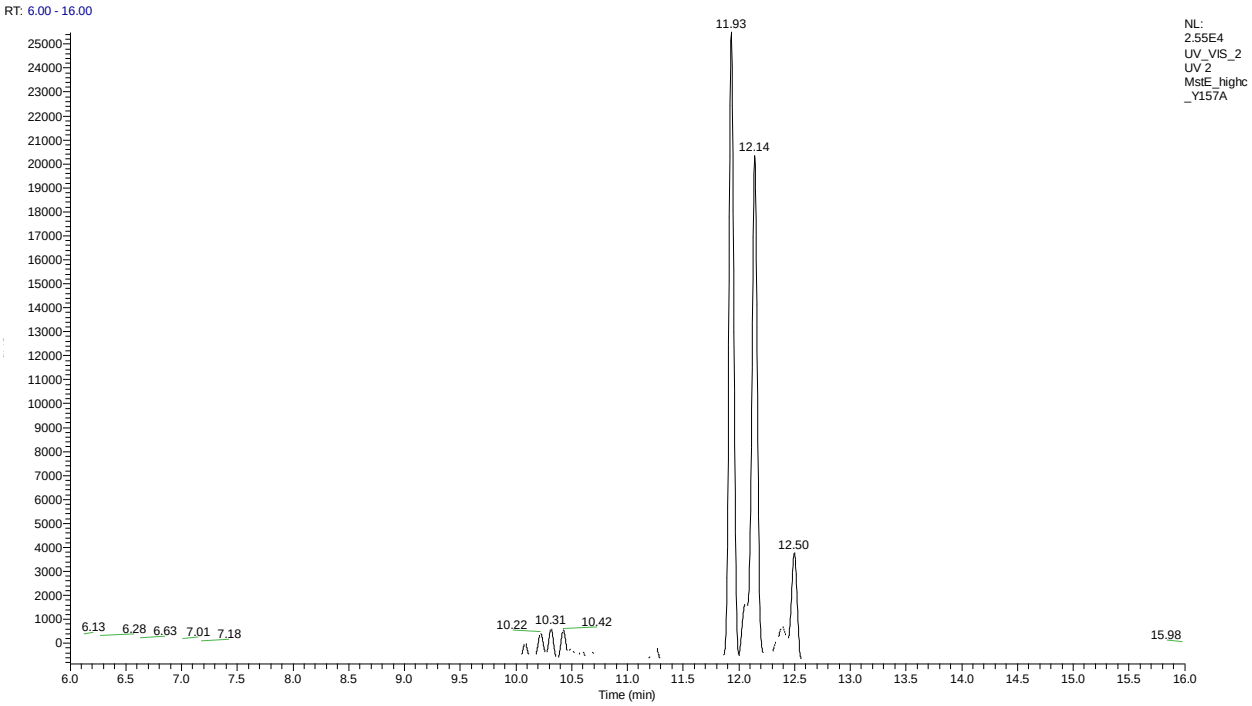

B)

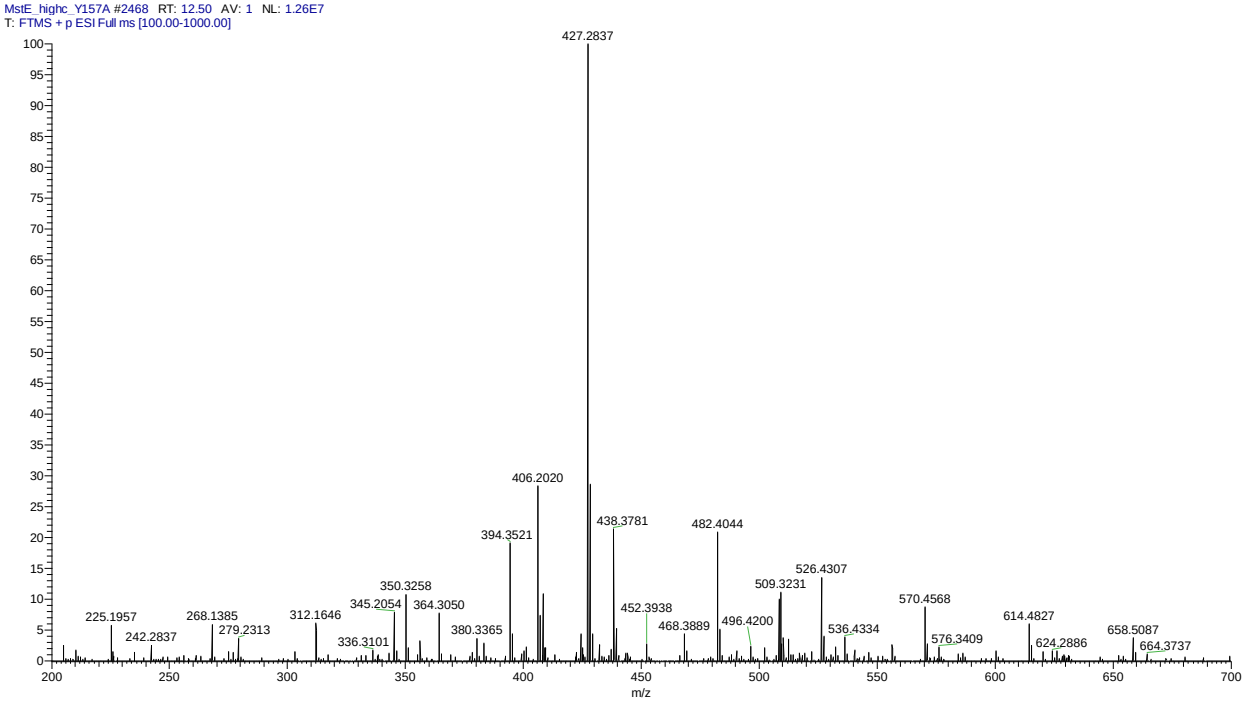

Supplementary Fig. 9. HPLC chromatogram and mass spectrum of merosterolic acid B (9).

(**A**) UV trace at 254 nm of the chromatogram of assays containing MstE Y157A and 3-geranylgeranyl-4,5-dihydroxybenzoic acid (GG-DHB, **3**). The three major peaks are merosterolic acid A (**2**) at 11.93 min, substrate **3** at 12.14 min and merosterolic acid B (**9**) at 12.50 min. (**B**) Mass spectrum of the peak for **9** at 12.50 min (*m/z* 427.2837 $[M+H]^+$).

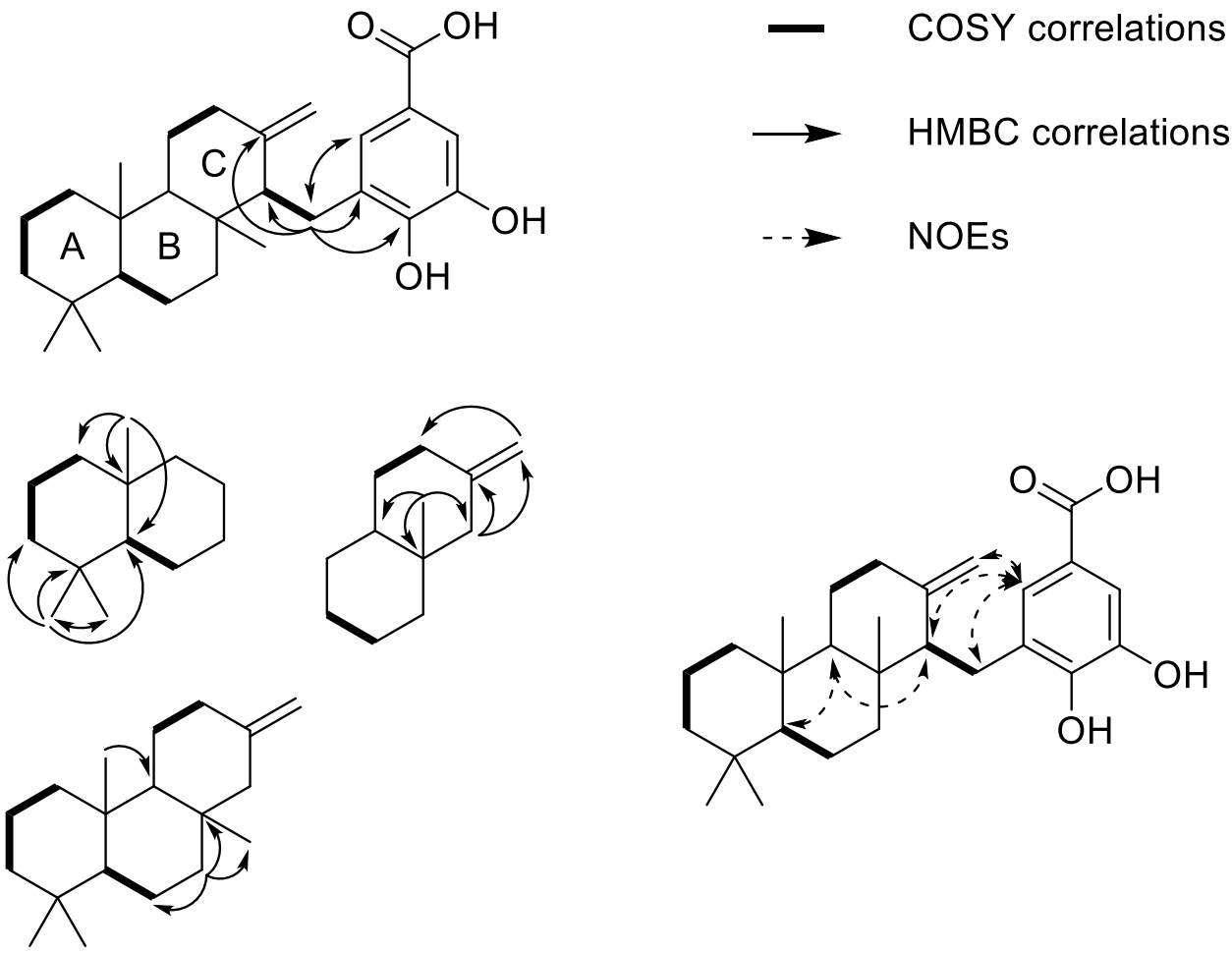

Supplementary Fig. 10. Key correlations identified in the NMR spectra of merosterolic acid B (9).

A)

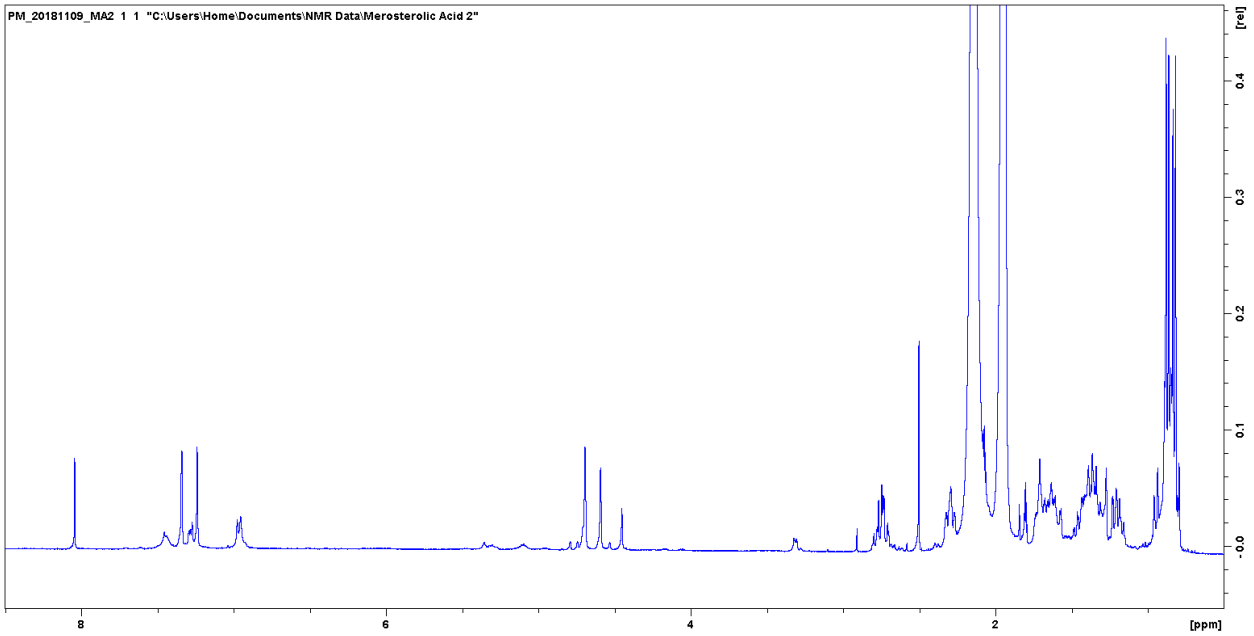

B)

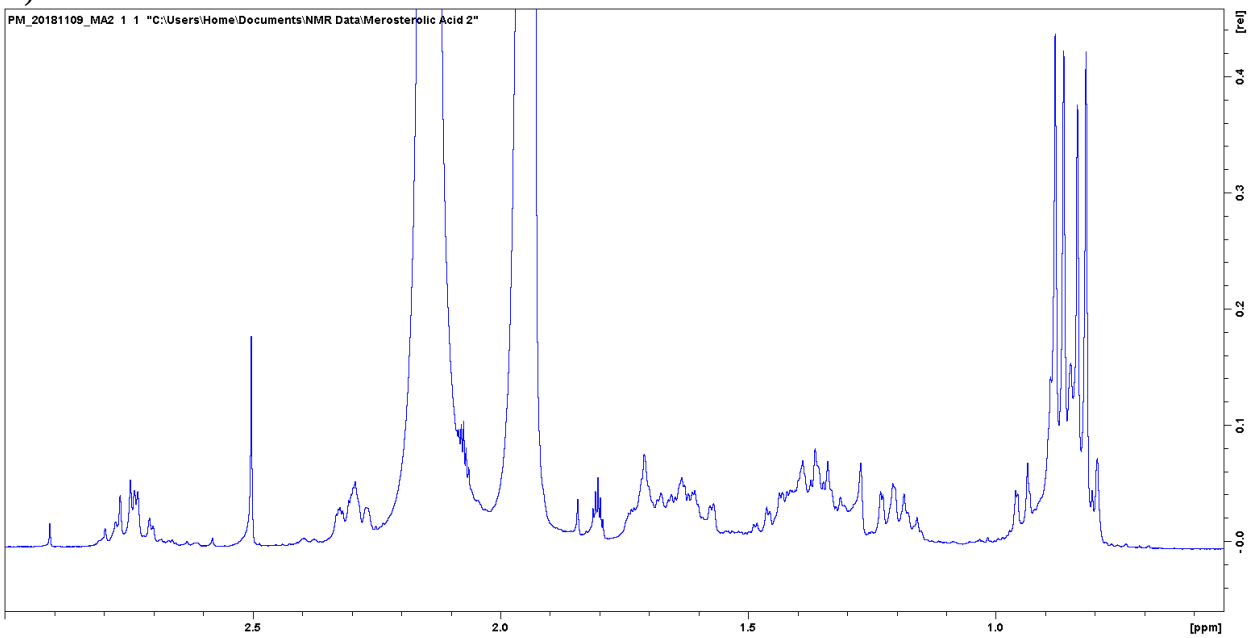

Supplementary Fig. 11. ^{1}H NMR spectrum of merosterolic acid B (9) in acetonitrile-d_3 (600 MHz). (**A**) Entire NMR spectrum. (**B**) Zoomed into the 0 – 3 ppm region.

A)

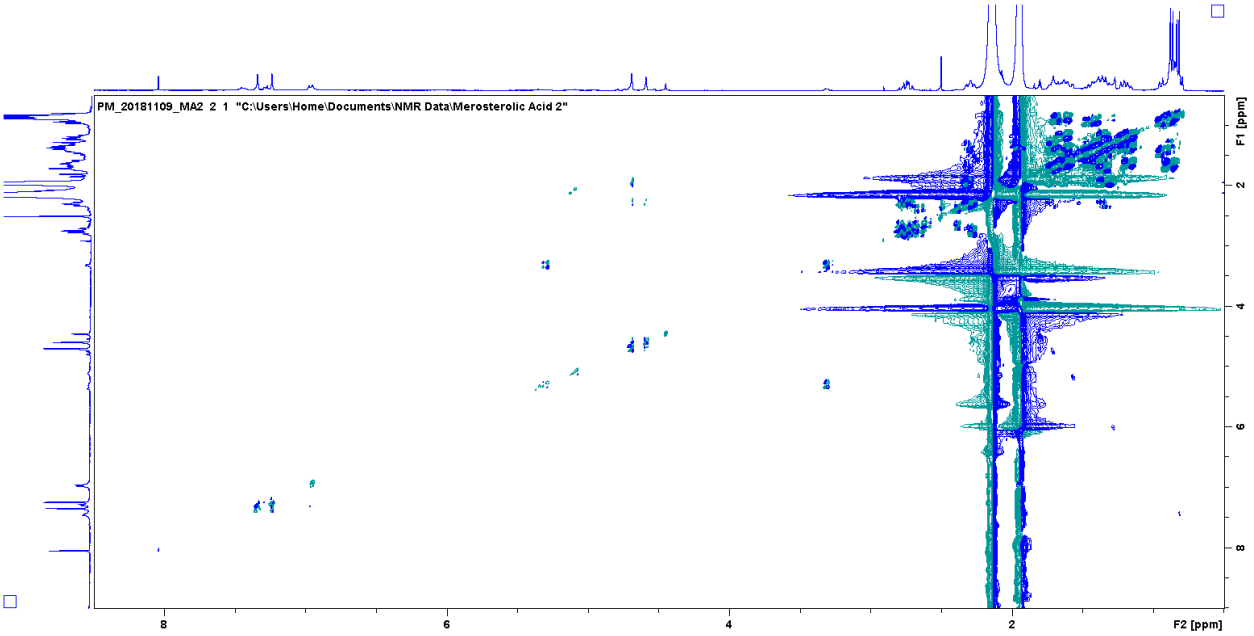

B)

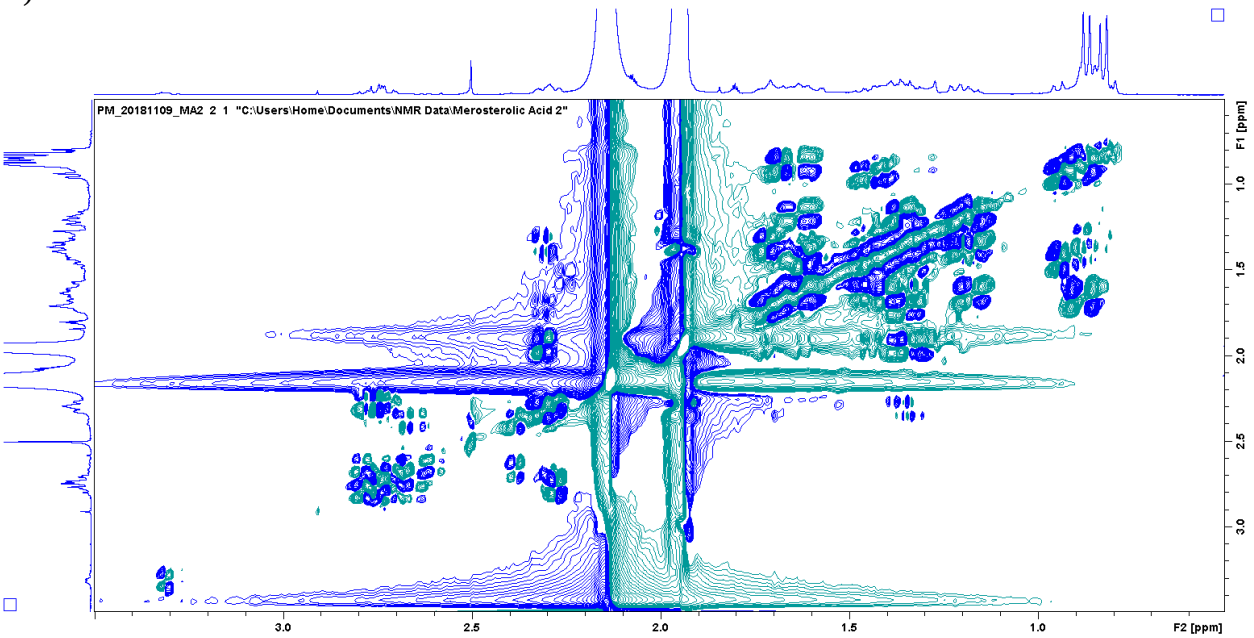

Supplementary Fig. 12. COSY spectrum of merosterolic acid B (9) in acetonitrile-d_3 (600 MHz). (**A**) Entire NMR spectrum. (**B**) Zoomed into the 0 – 3 ppm region.

A)

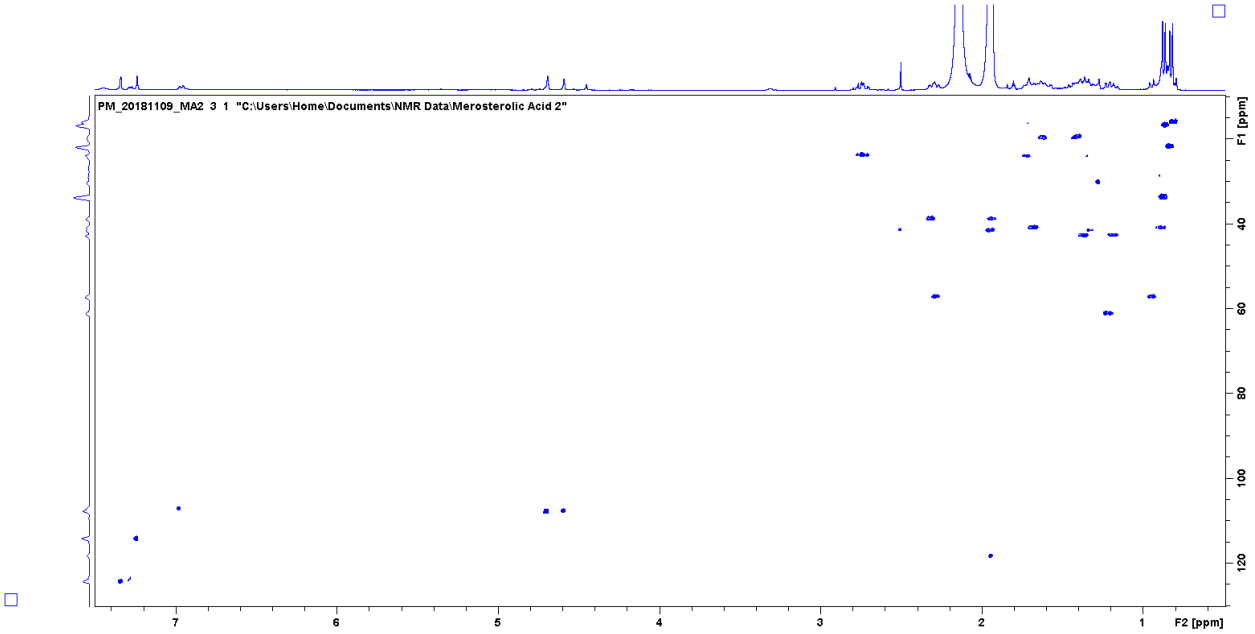

B)

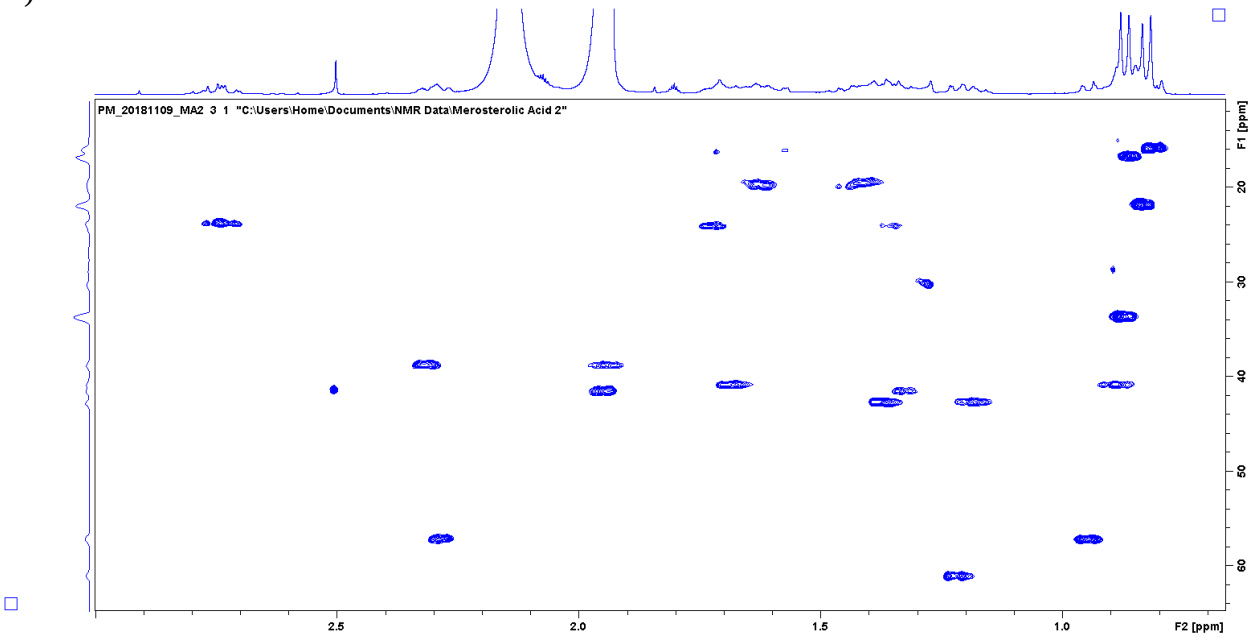

Supplementary Fig. 13. HSQC spectrum of merosterolic acid B (9) in acetonitrile-d_3 (600 MHz). (**A**) Entire NMR spectrum. (**B**) Zoomed into the 0 – 3 ppm and 0-60 ppm regions.

A)

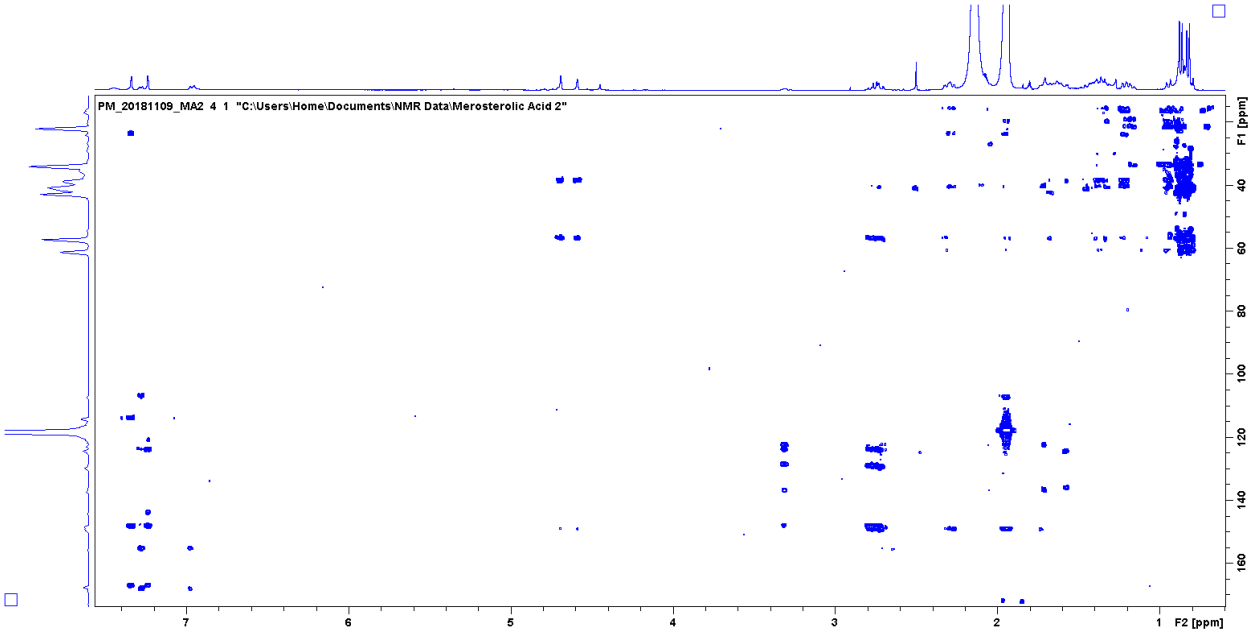

B)

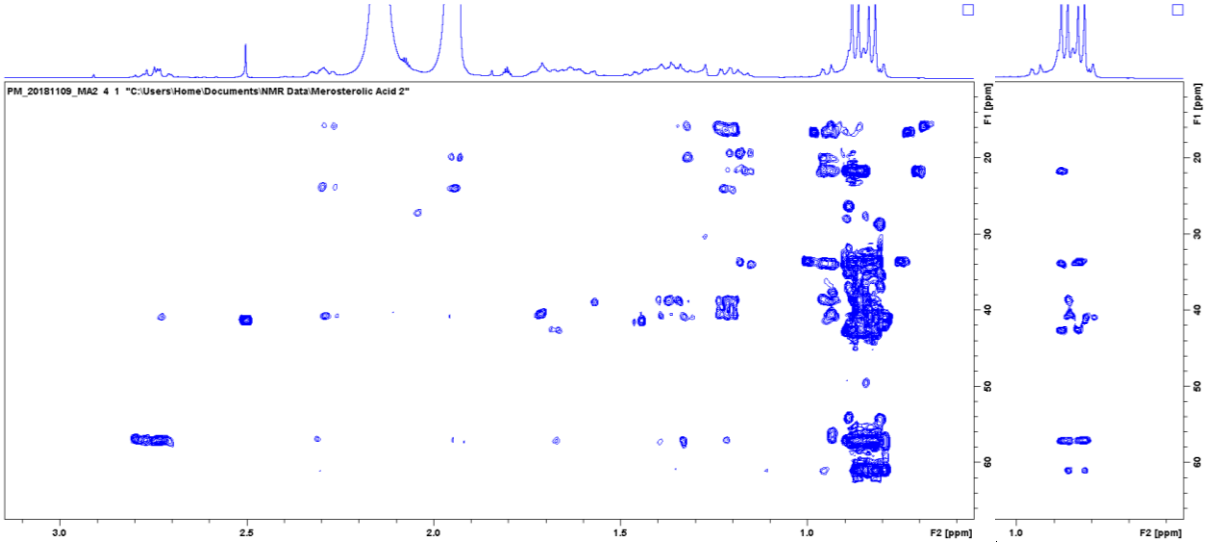

Supplementary Fig. 14. HMBC spectrum of merosterolic acid B (9) in acetonitrile-d_3 (600 MHz).
(**A**) Entire NMR spectrum. (**B**) Left: Zoomed into the 0 – 3 ppm and 0-60 ppm regions. Right: Zoomed into HMBC signals of methyl groups.

A)

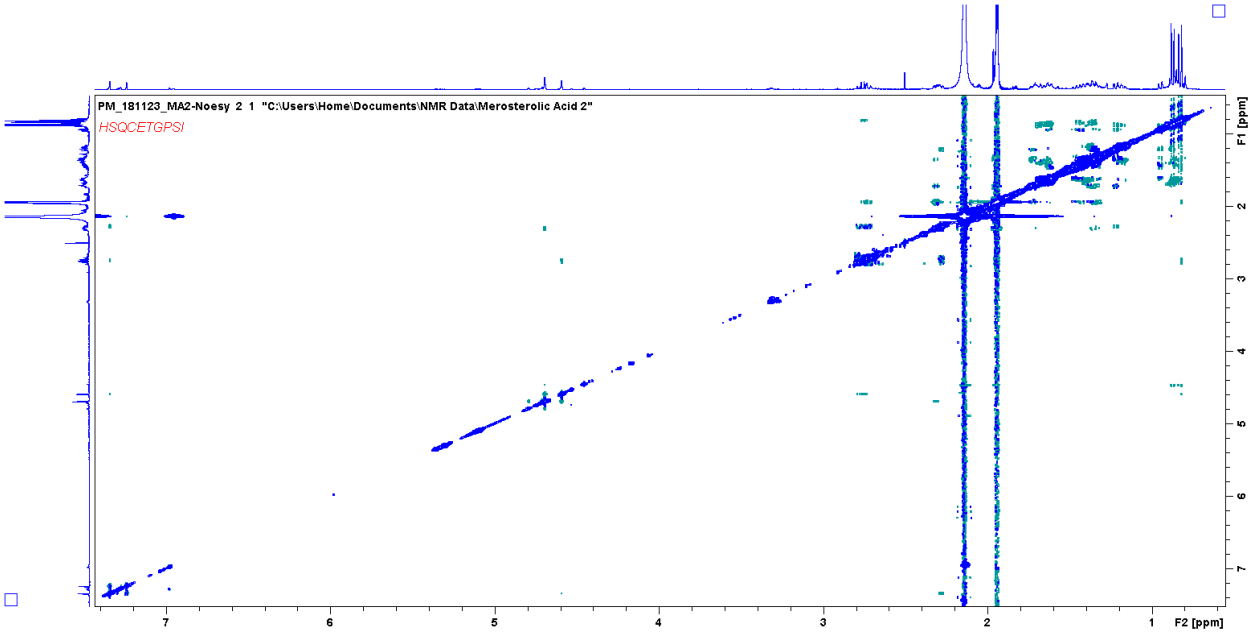

B)

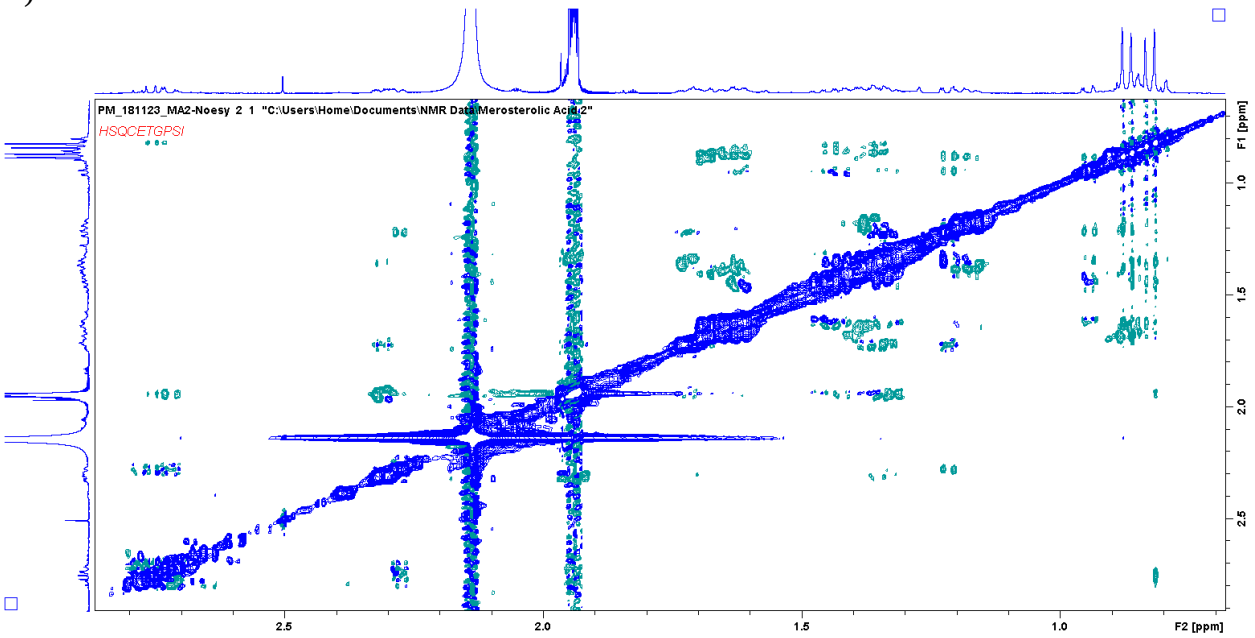

Supplementary Fig. 15. NOESY spectrum of merosterolic acid B (9) in acetonitrile-d_3 (600 MHz). (**A**) Entire NMR spectrum. (**B**) Zoomed into the 0 – 3 ppm region.

A)

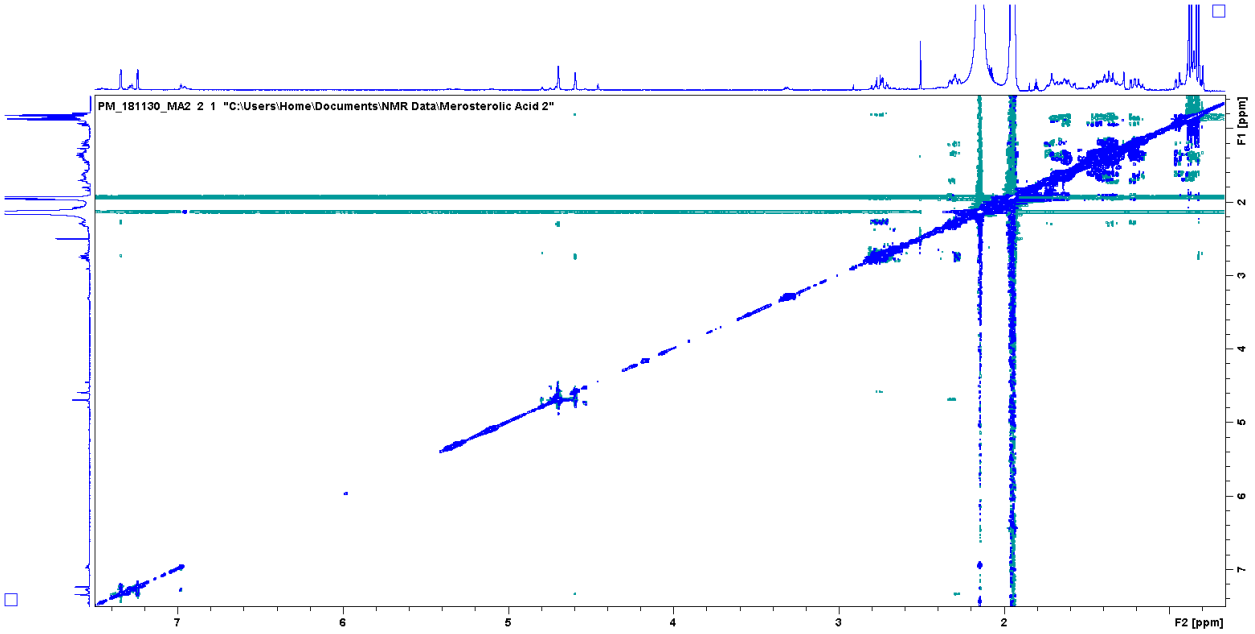

B)

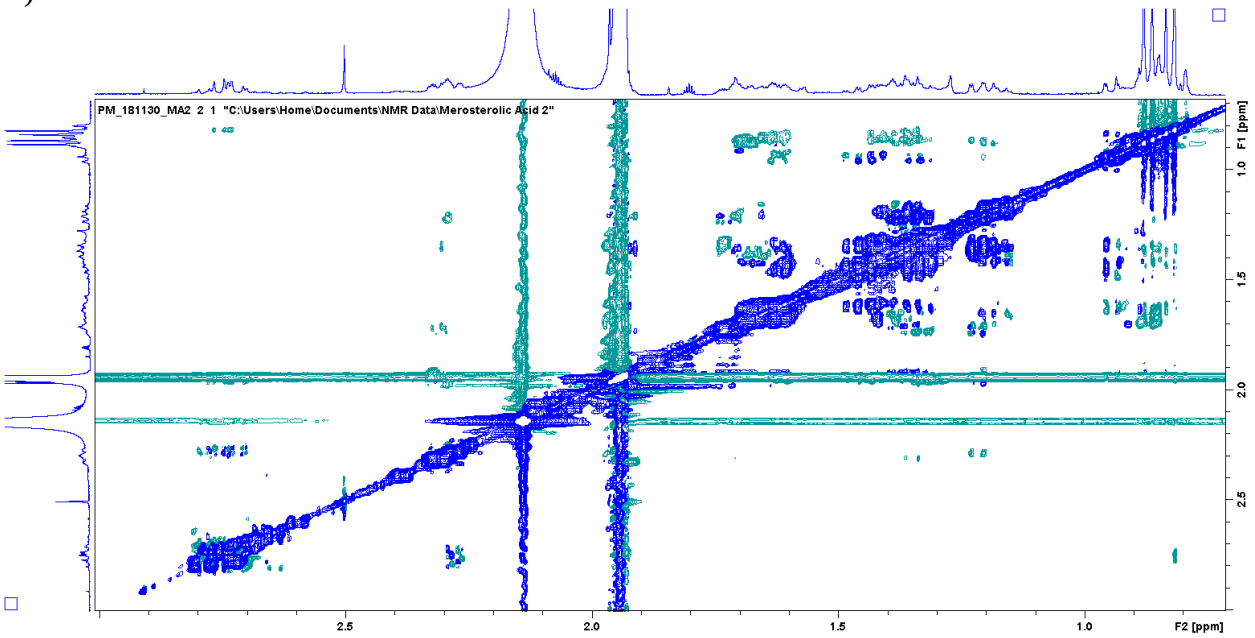

Supplementary Fig. 16. ROESY spectrum of merosterolic acid B (9) in acetonitrile-d_3 (600 MHz). (**A**) Entire NMR spectrum. (**B**) Zoomed into the 0 – 3 ppm region.

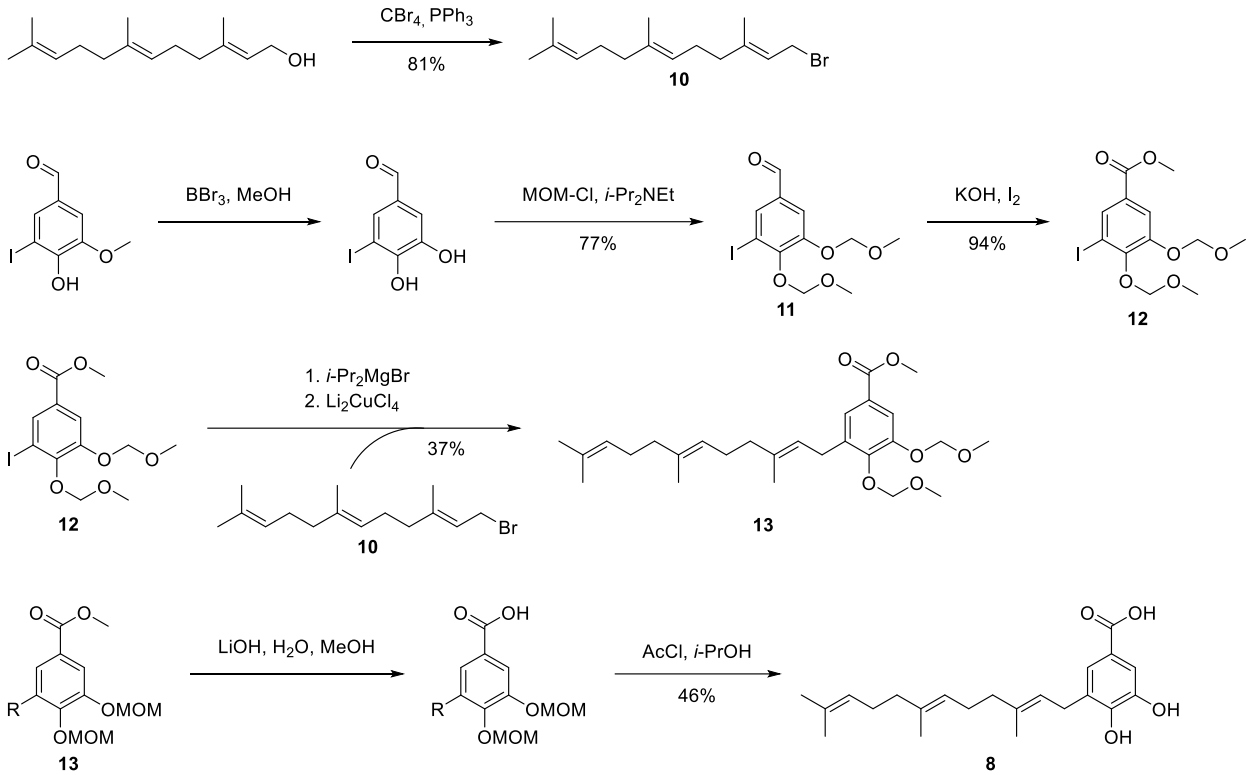

Supplementary Fig. 17. Synthesis of 3-farnesyl-4,5-dihydroxybenzoic acid (8).

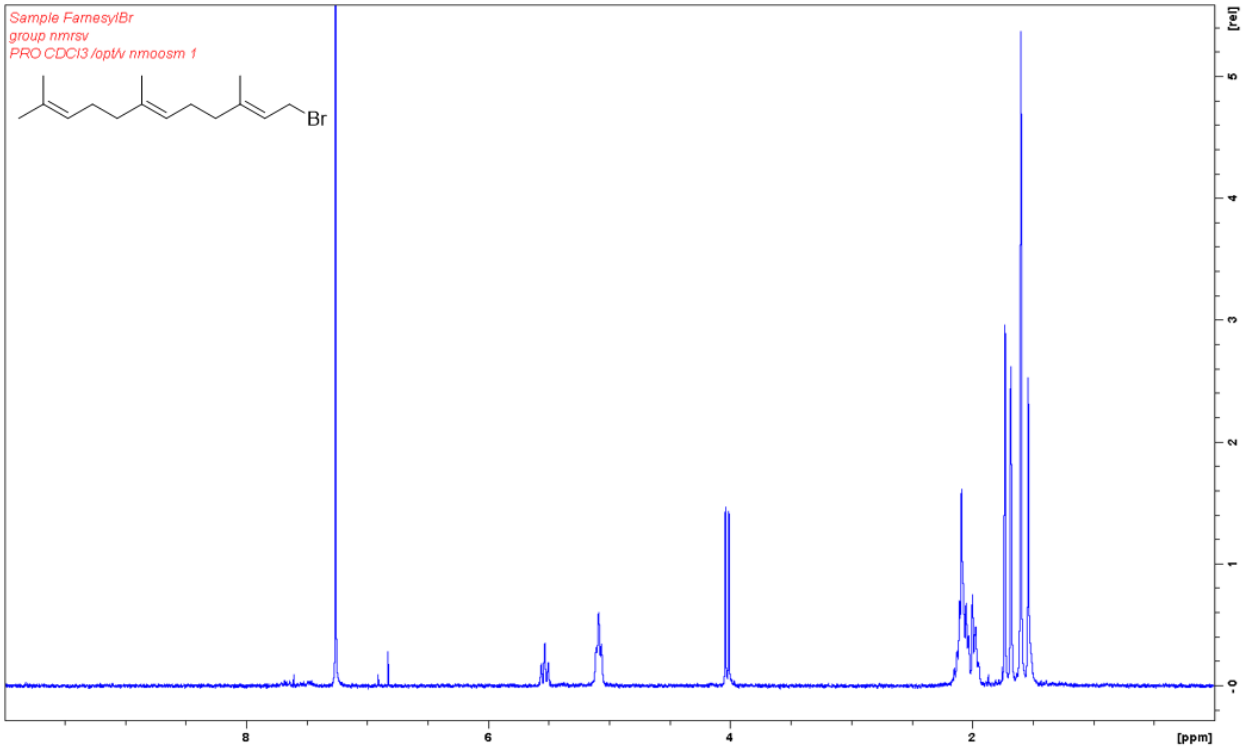

Supplementary Fig. 18. ^{1}H-NMR of (*E*, *E*)-farnesylbromide (10) in $CDCl_3$ (300 MHz).

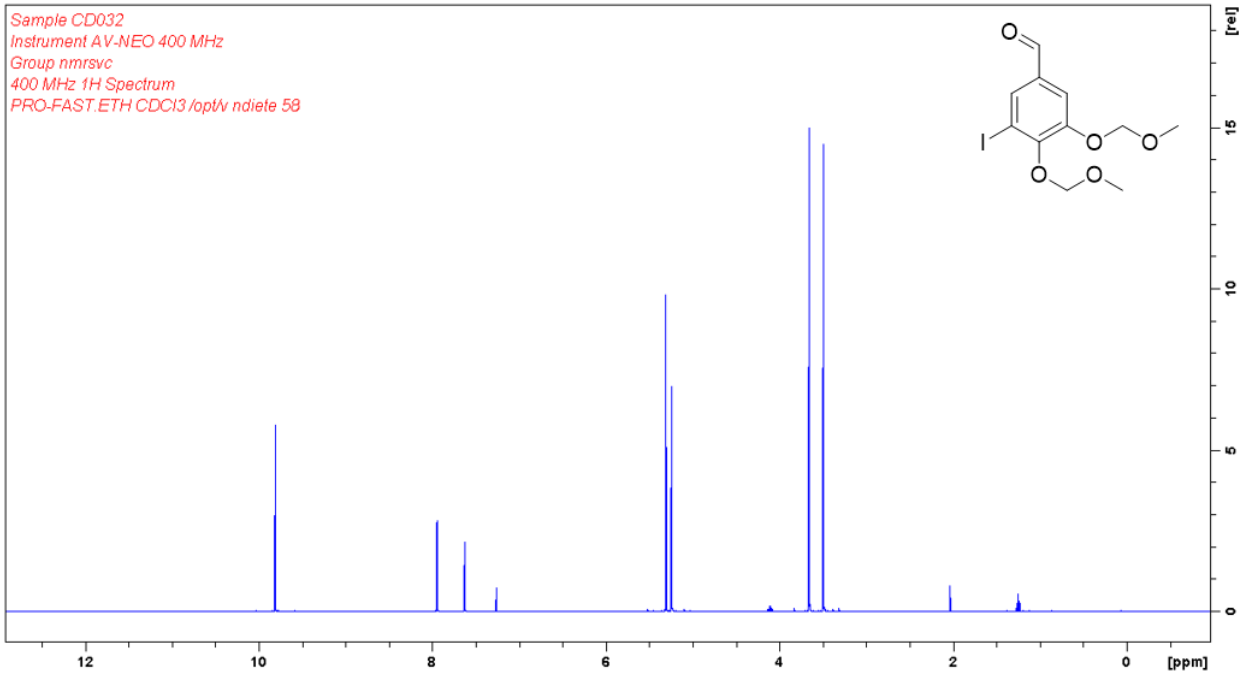

Supplementary Fig. 19. ^{1}H-NMR of 3-iodo-4,5-bis(methoxymethoxy)benzaldehyde (11) in $CDCl_3$ (400 MHz).

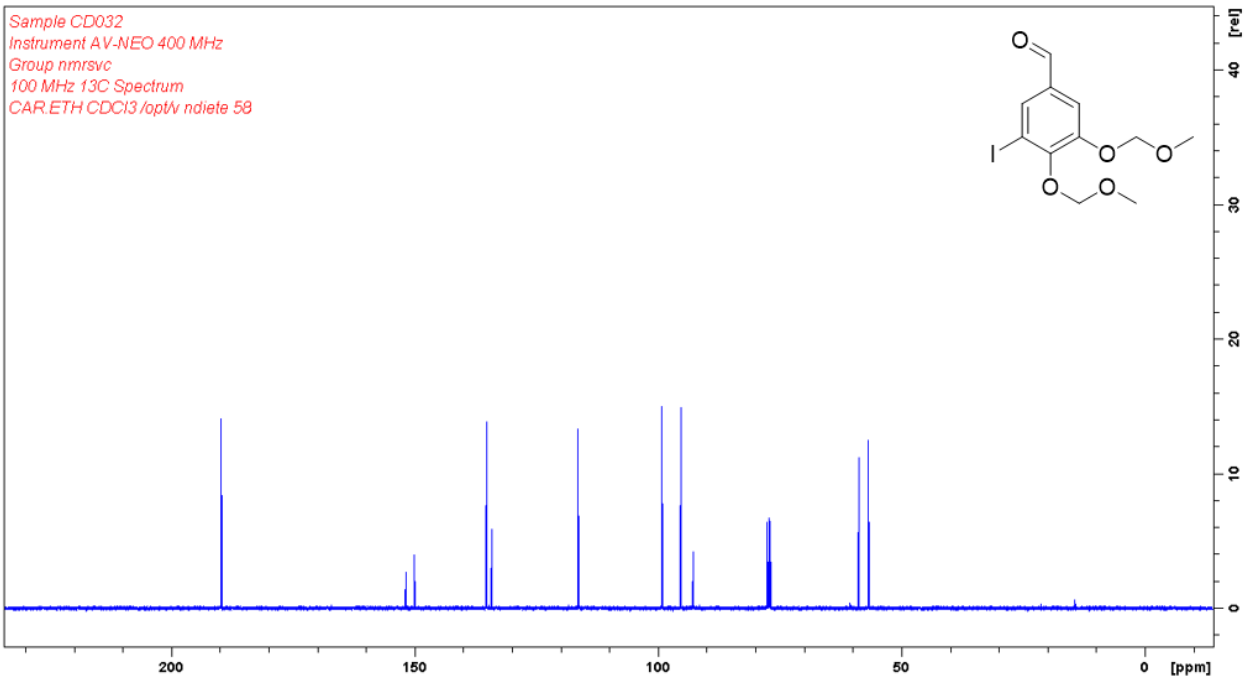

Supplementary Fig. 20. ^{13}C-NMR of 3-iodo-4,5-bis(methoxymethoxy)benzaldehyde (11) in $CDCl_3$ (400 MHz).

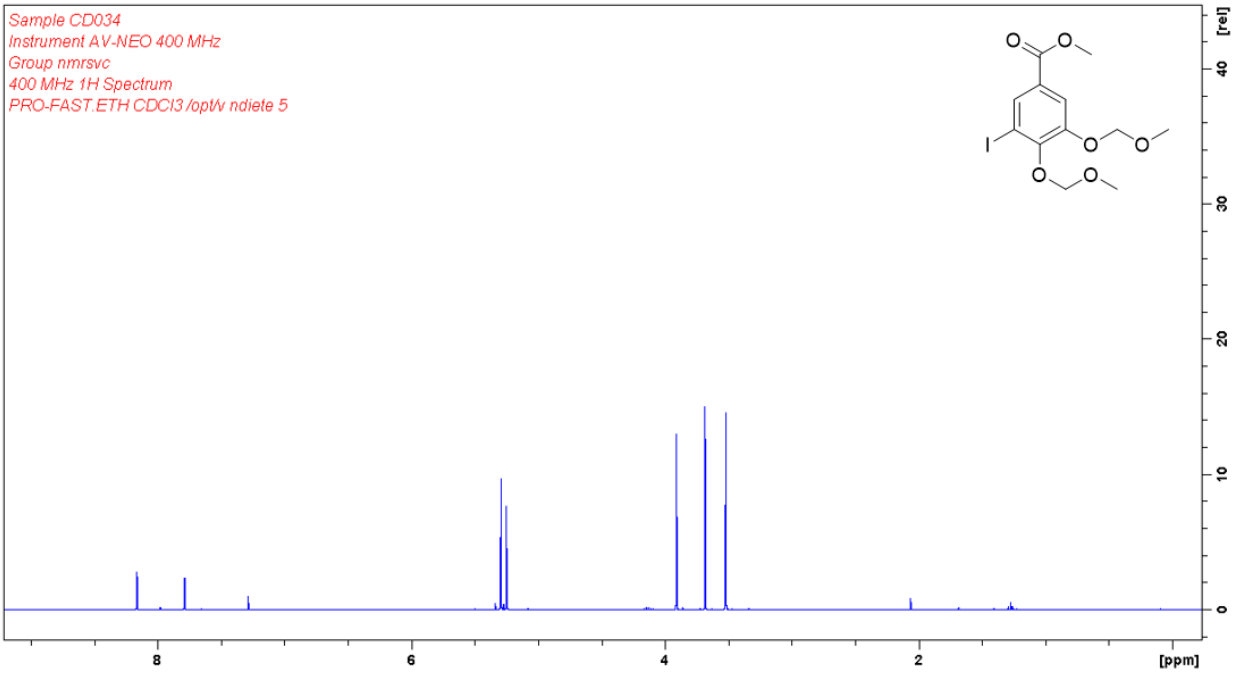

Supplementary Fig. 21. ^{1}H-NMR of methyl 3-iodo-4,5-bis(methoxymethoxy)benzoate (12) in $CDCl_3$ (400 MHz).

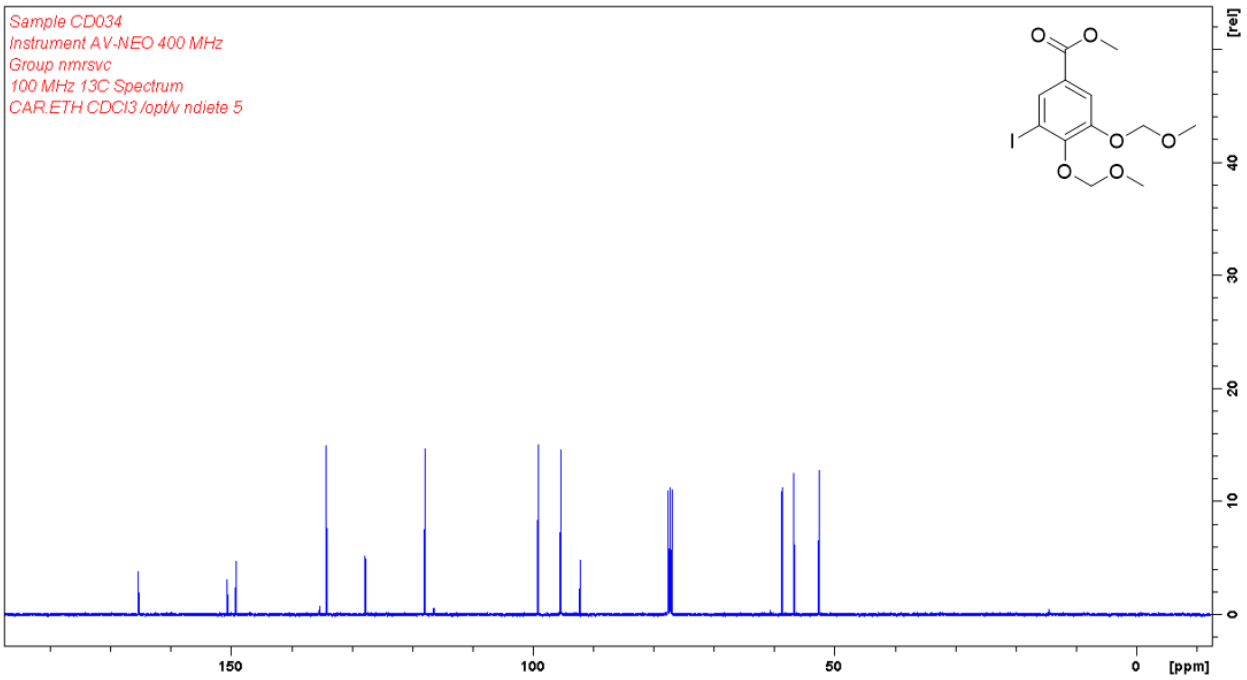

Supplementary Fig. 22. ^{13}C-NMR of methyl 3-iodo-4,5-bis(methoxymethoxy)benzoate (12) in $CDCl_3$ (400 3MHz).

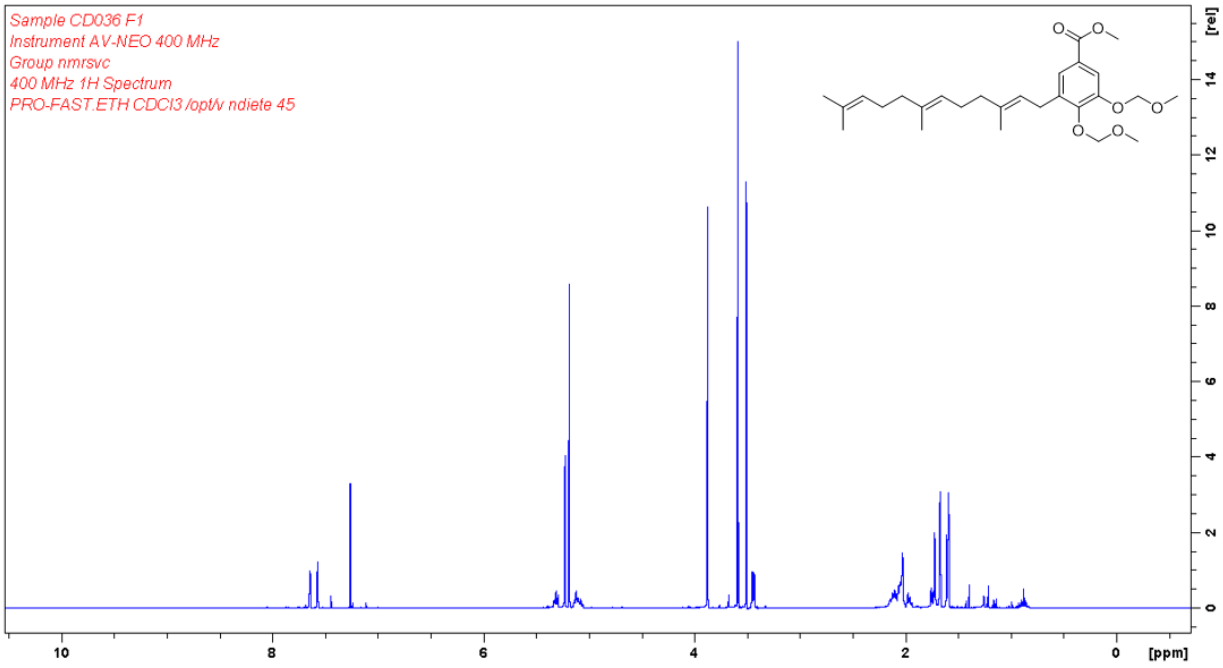

Supplementary Fig. 23. ^{1}H-NMR of 3,4-bis(methoxymethoxy)-5-((2E,6E)-3,7,11-trimethyldodeca-2,6,10-trien-1-yl)benzoate (13) in $CDCl_3$ (400 MHz).

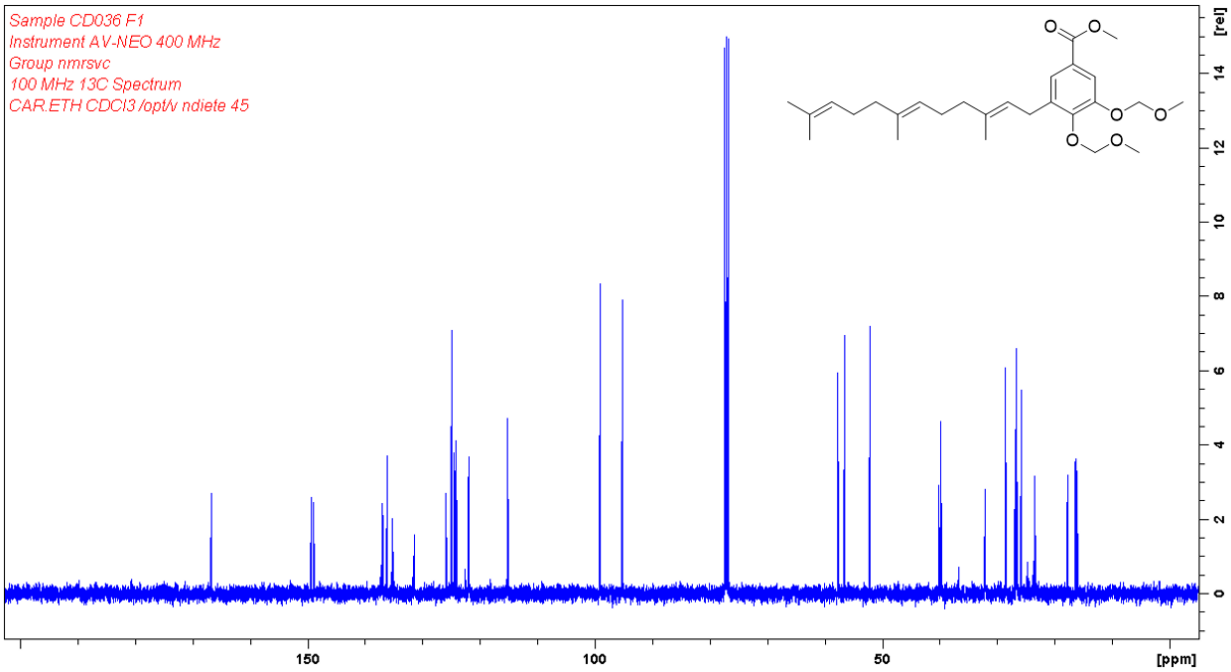

Supplementary Fig. 24. ^{13}C-NMR of 3,4-bis(methoxymethoxy)-5-((2E,6E)-3,7,11-trimethyldodeca-2,6,10-trien-1-yl)benzoate (13) in $CDCl_3$ (400 MHz).

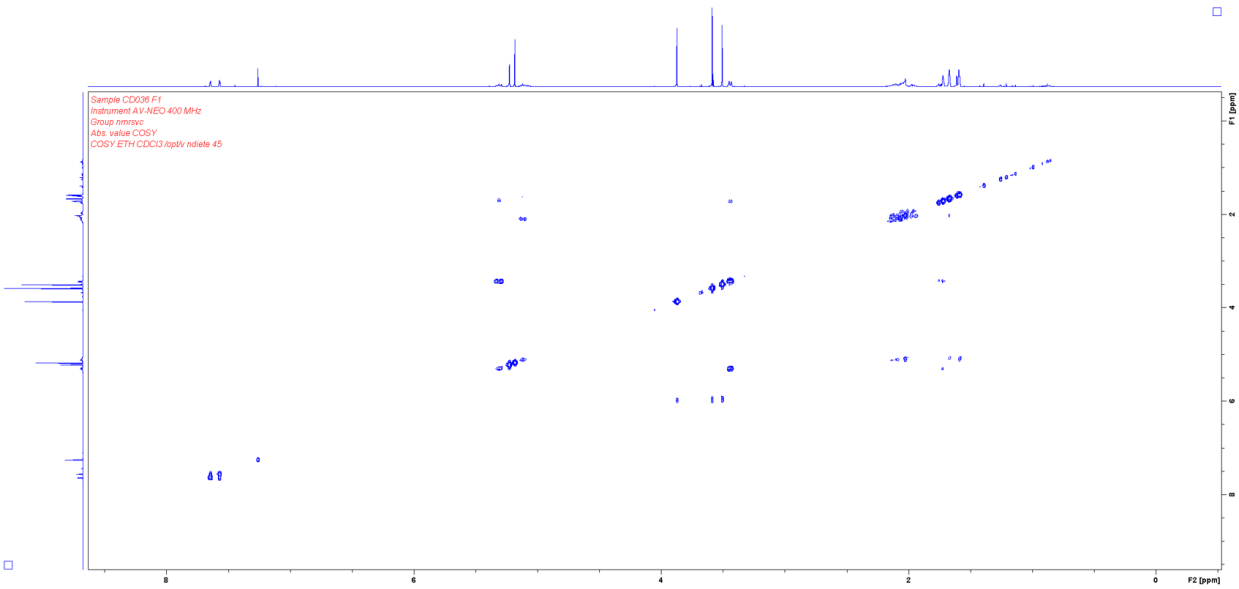

Supplementary Fig. 25. COSY spectrum of 3,4-bis(methoxymethoxy)-5-((2E,6E)-3,7,11-trimethyldodeca-2,6,10-trien-1-yl)benzoate (13) in $CDCl_3$ (400 MHz).

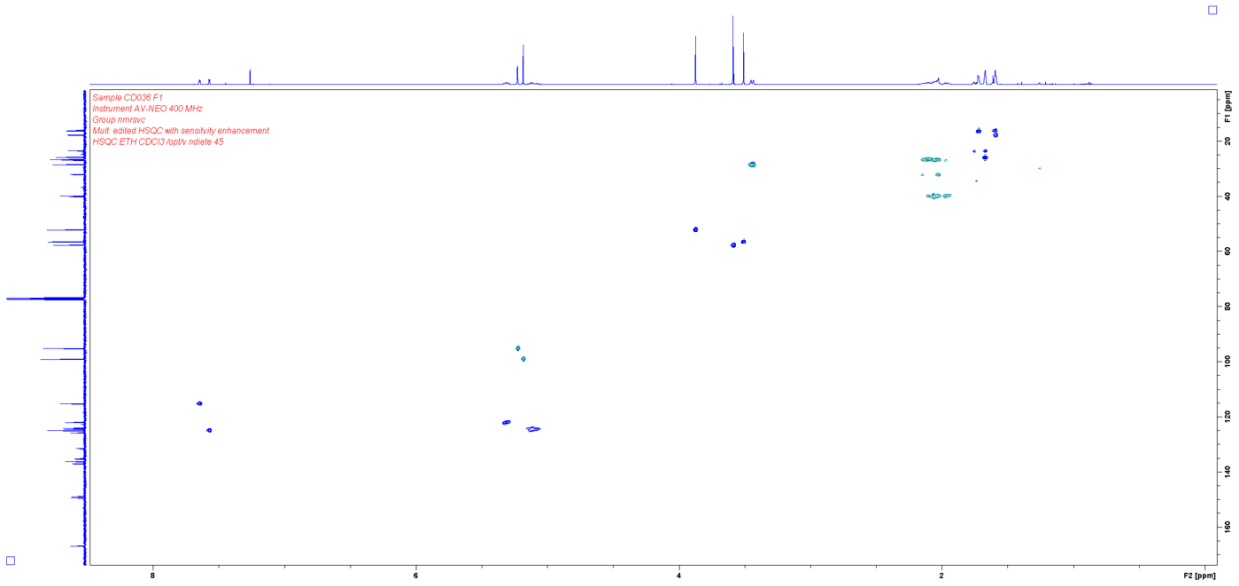

Supplementary Fig. 26. HSQC spectrum of 3,4-bis(methoxymethoxy)-5-((2E,6E)-3,7,11-trimethyldodeca-2,6,10-trien-1-yl)benzoate (13) in $CDCl_3$ (400 MHz).

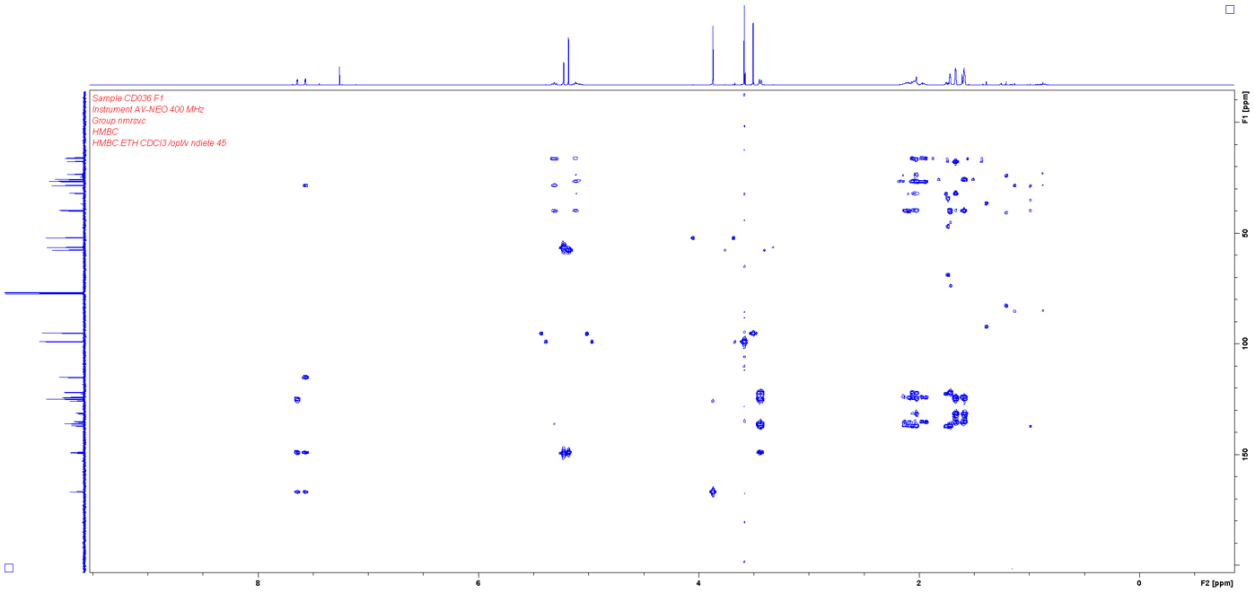

Supplementary Fig. 27. HMBC spectrum of 3,4-bis(methoxymethoxy)-5-((2E,6E)-3,7,11-trimethyldodeca-2,6,10-trien-1-yl)benzoate (13) in $CDCl_3$ (400 MHz).

A)

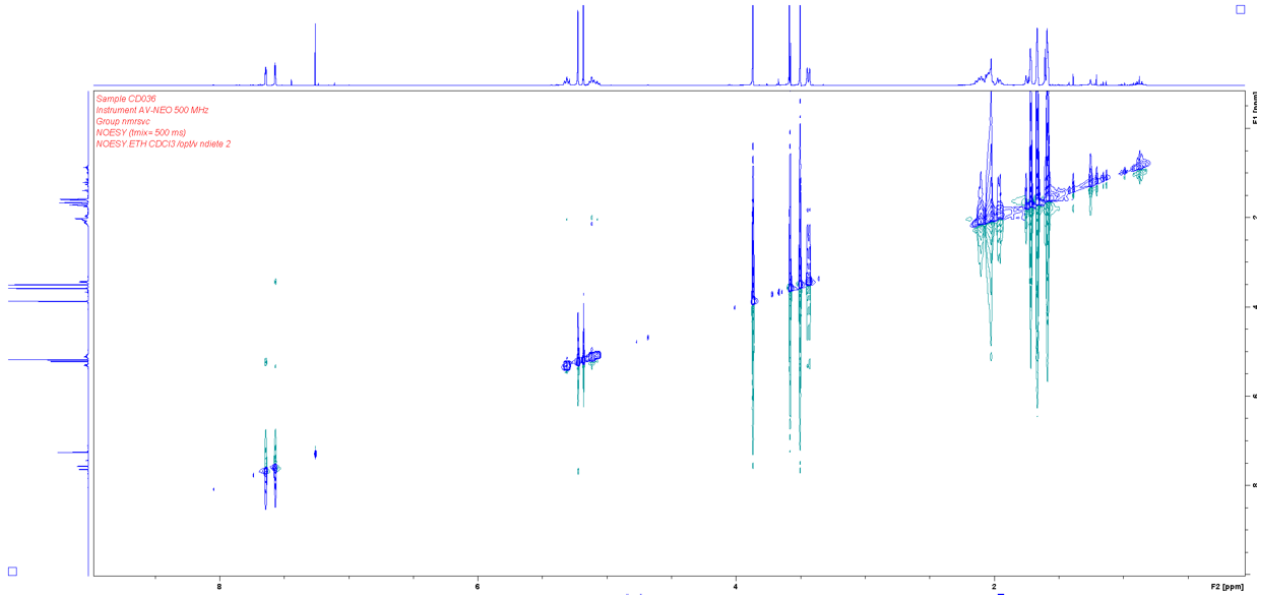

B)

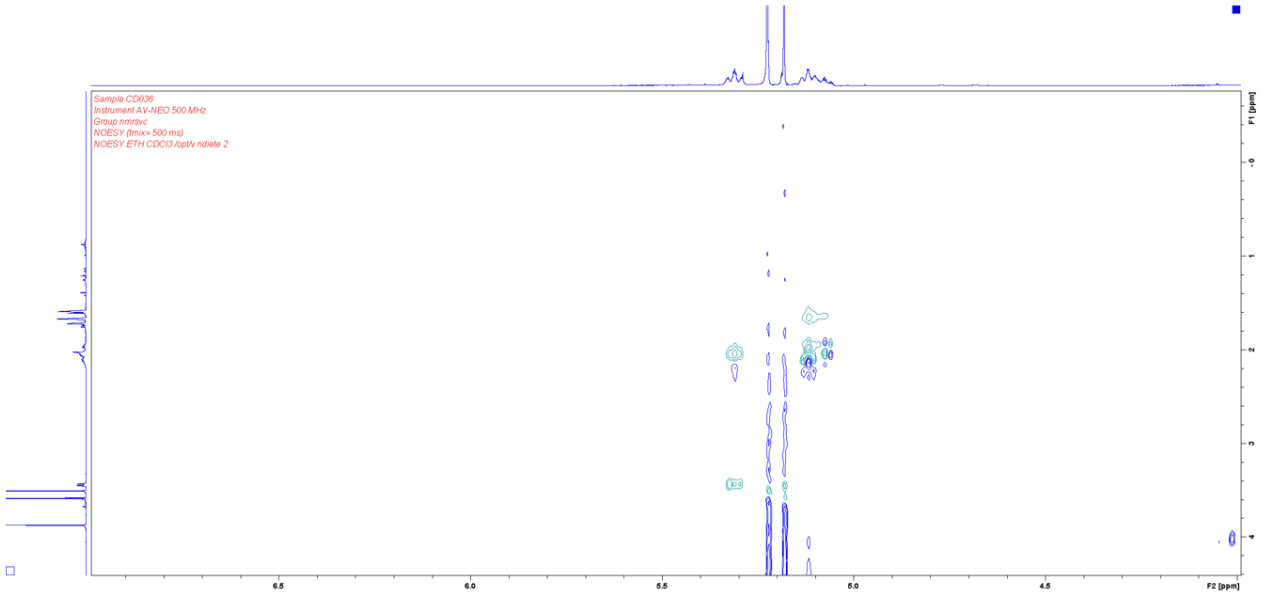

Supplementary Fig. 28. NOESY spectrum of 3,4-bis(methoxymethoxy)-5-((2E,6E)-3,7,11-trimethyldodeca-2,6,10-trien-1-yl)benzoate (13) in $CDCl_3$ (500 MHz).
(A) Entire NMR spectrum. **(B)** Zoomed into the 4 – 7 ppm region.

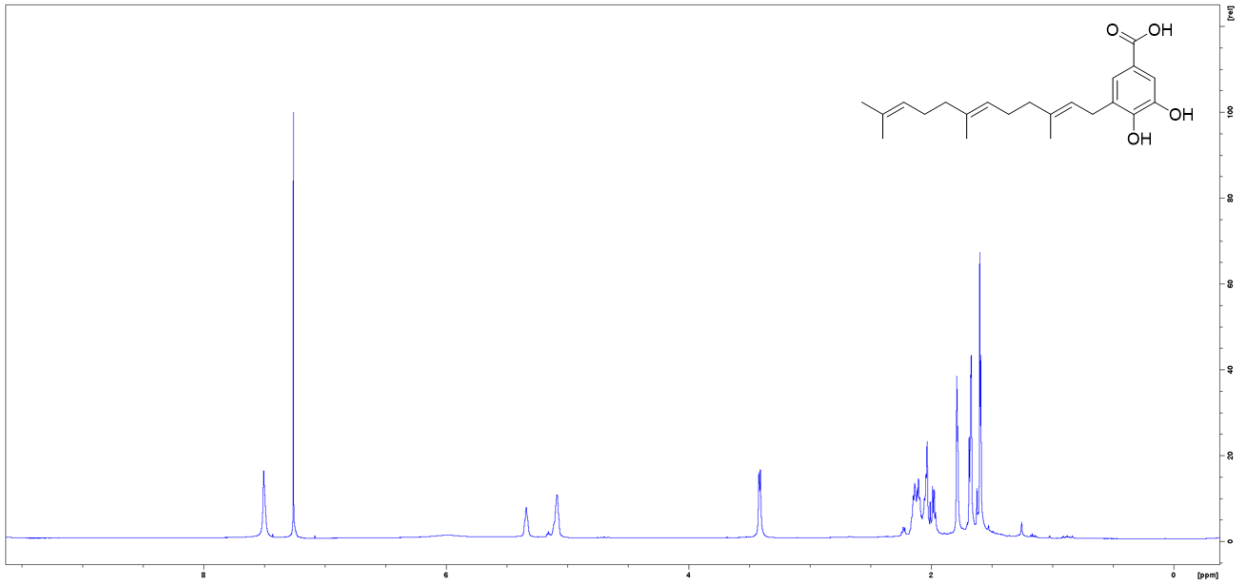

Supplementary Fig. 29. ^{1}H-NMR of 3-farnesyl-4,5-dihydroxybenzoic acid (8) in $CDCl_3$ (600 MHz).

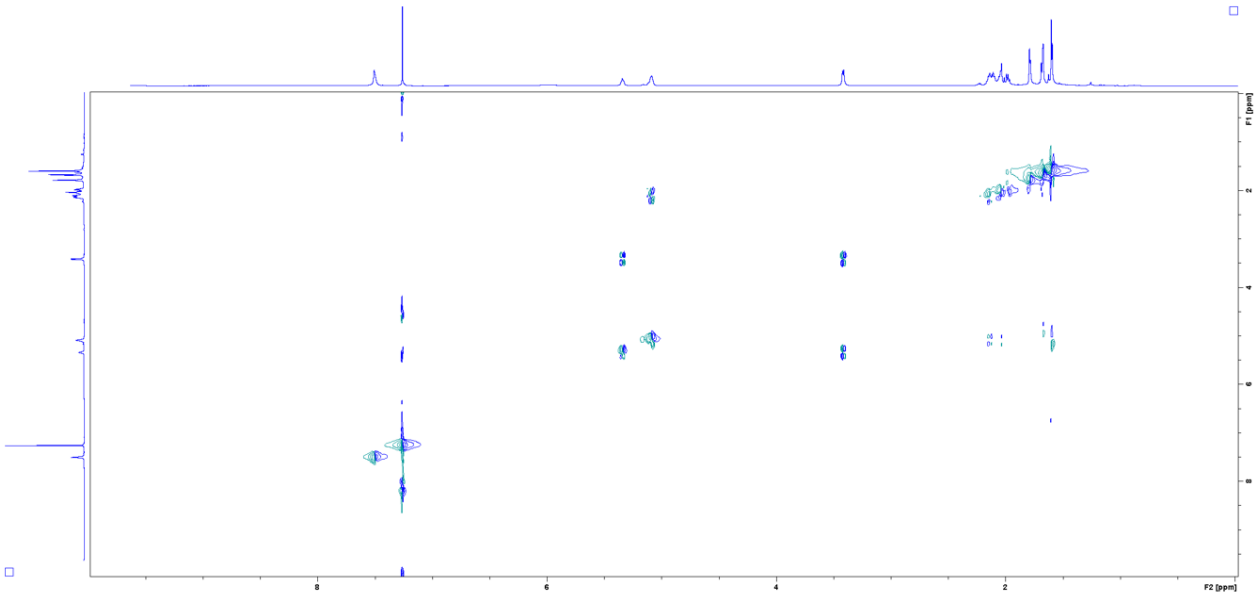

Supplementary Fig. 30. COSY spectrum of 3-farnesyl-4,5-dihydroxybenzoic acid (8) in $CDCl_3$ (600 MHz).

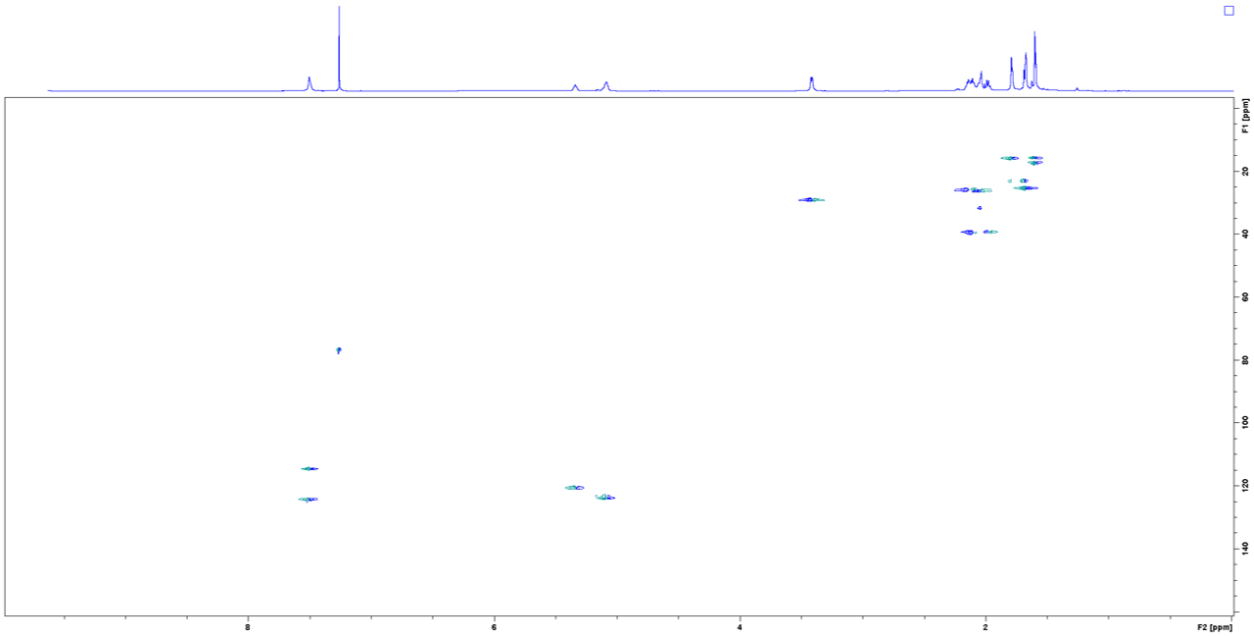

Supplementary Fig. 31. HSQC spectrum of 3-farnesyl-4,5-dihydroxybenzoic acid (8) in $CDCl_3$ (600 MHz).

A)

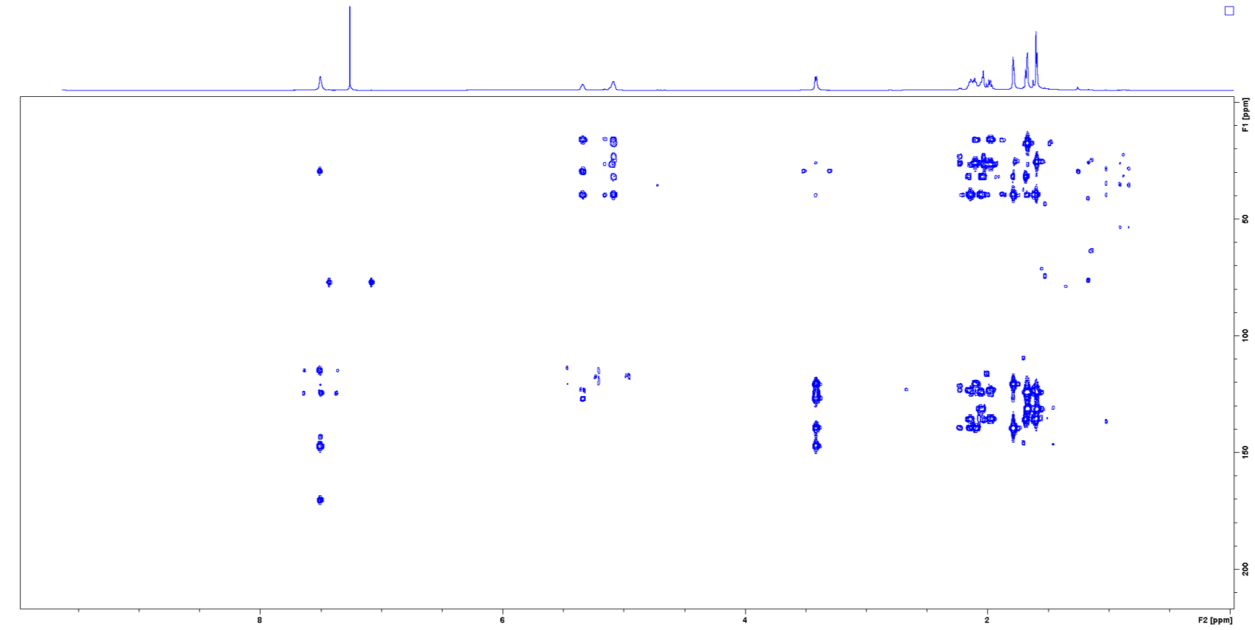

B)

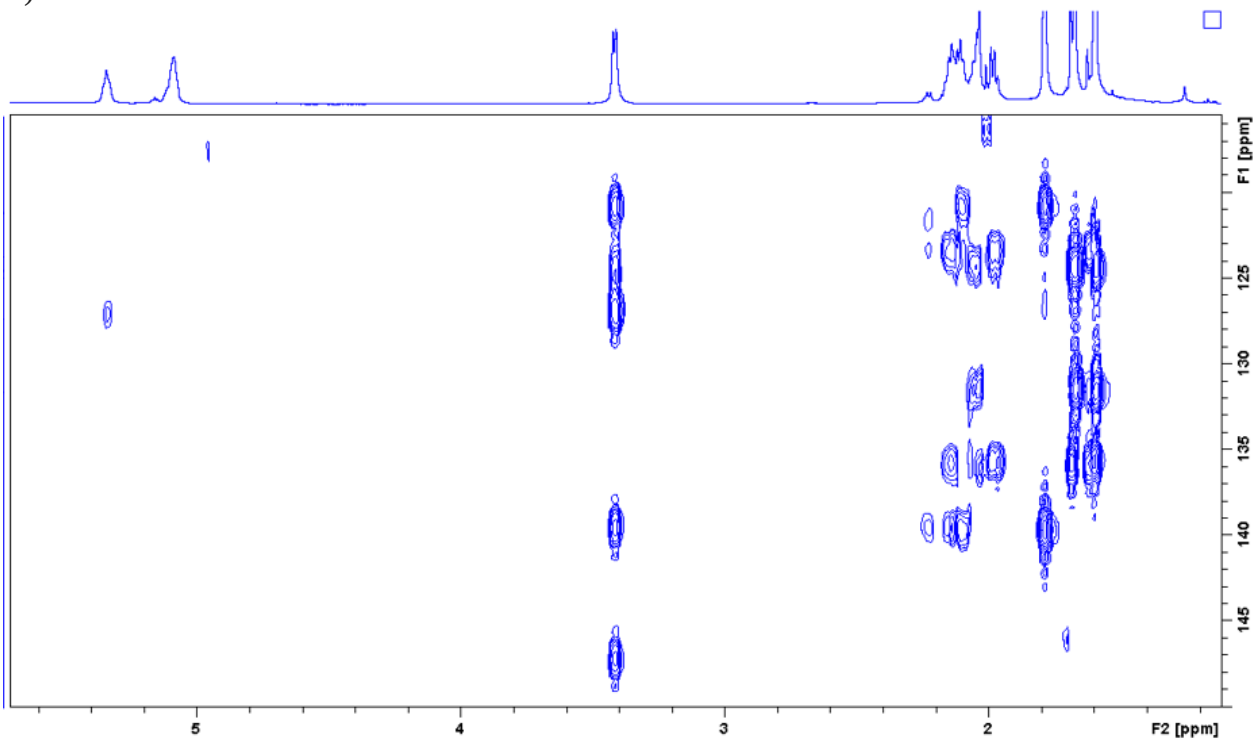

C)

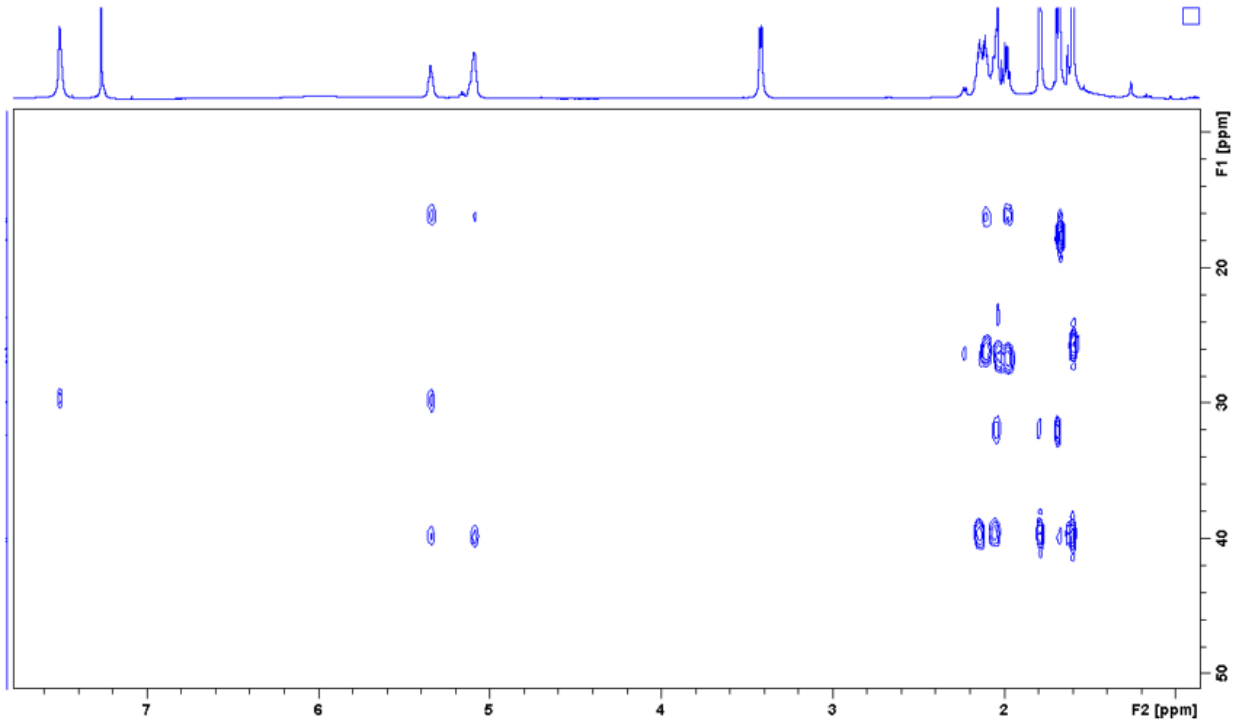

Supplementary Fig. 32. HMBC spectrum of of 3-farnesyl-4,5-dihydroxybenzoic acid (8) in $CDCl_3$ (600 MHz).
(A) Entire NMR spectrum. **(B)** Zoom in on 1 - 6 ppm and 115 - 150 ppm regions. **(C)** Zoom in on 1 - 8 ppm and 10 - 50 ppm regions.

A)

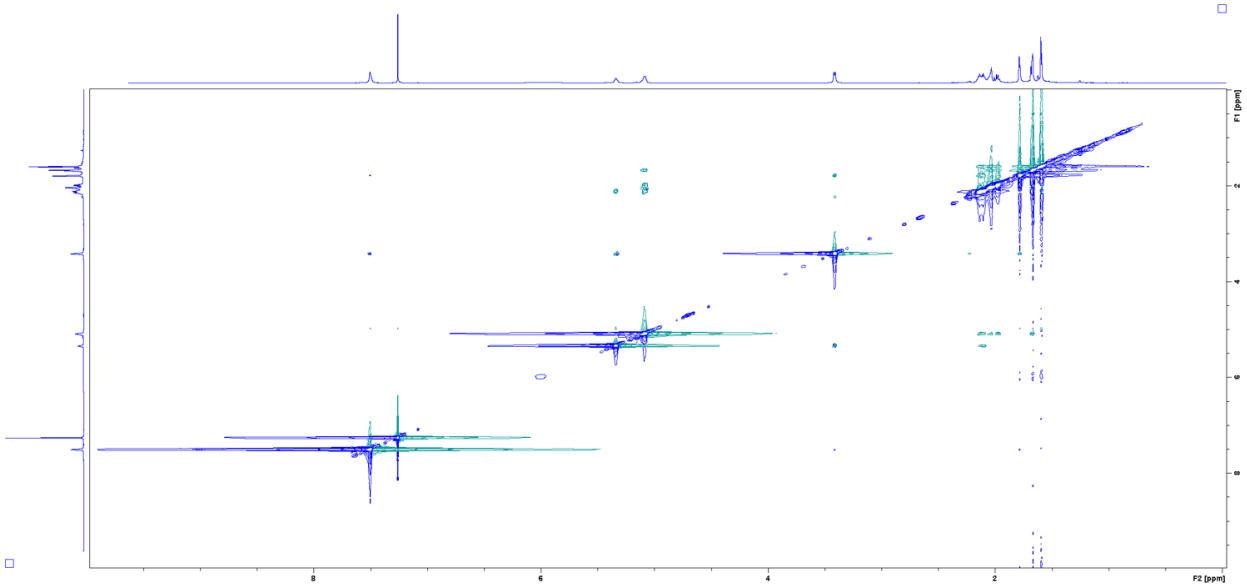

B)

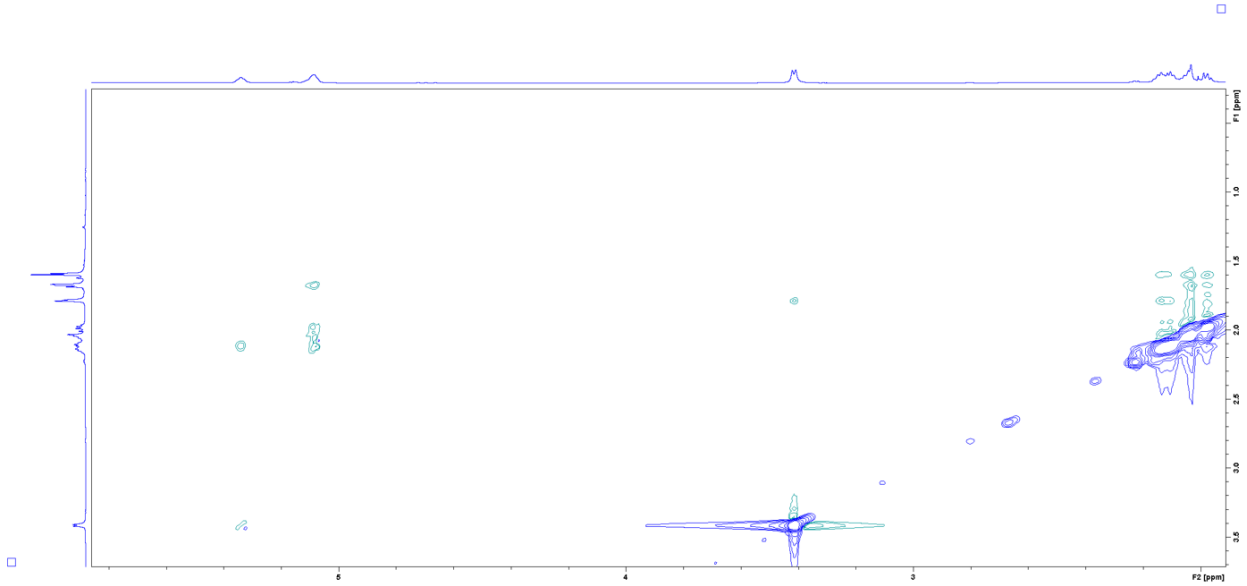

Supplementary Fig. 33. NOESY spectrum of of 3-farnesyl-4,5-dihydroxybenzoic acid (8) in $CDCl_3$ (600 MHz).
(A) Entire NMR spectrum. **(B)** Zoom in Zoom in on 2 - 6 ppm and 0.5 - 3.7 ppm regions.

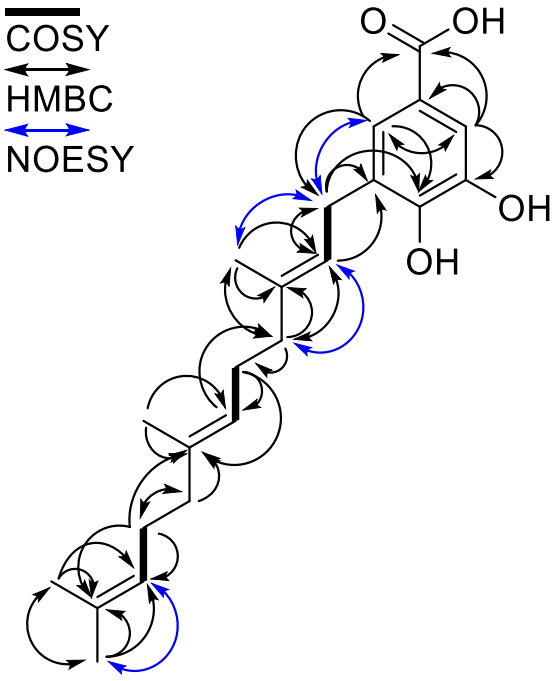

Supplementary Fig. 34. Key correlations identified in the 2D NMR spectra of 3-farnesyl-4,5-dihydroxybenzoic acid (8).

A)

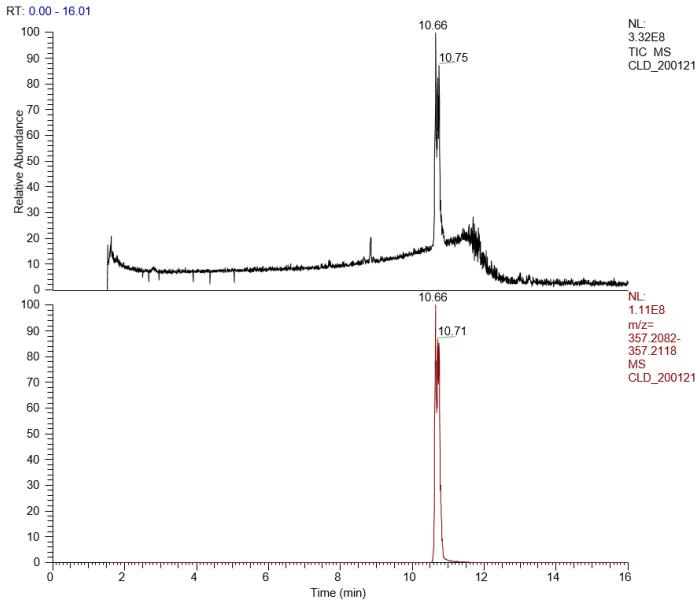

B)

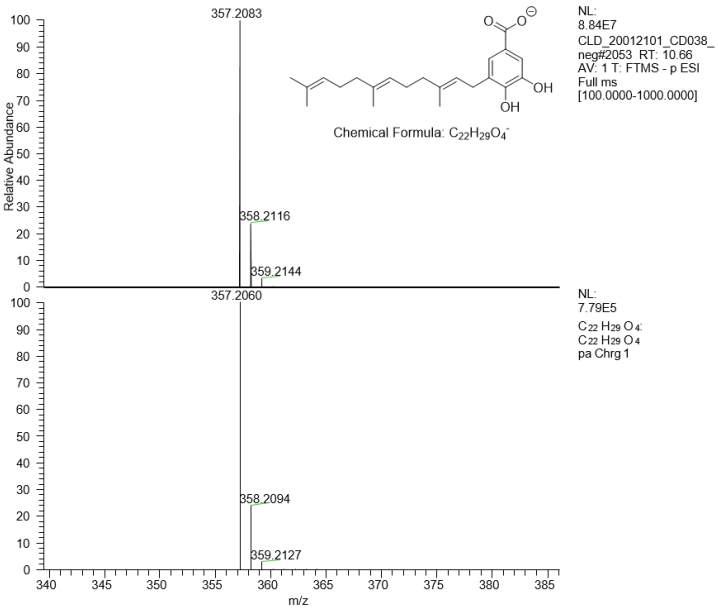

Supplementary Fig. 35. HR-LCMS data of 3-farnesyl-4,5-dihydroxybenzoic acid (8).

(A) Chromatogram (upper trace) and extracted ion chromatogram (*m/z* 357.2082 - 357.2118) (lower trace) **(B)** Mass spectrum of the peak at 10.66 min retention time (*m/z* 357.2083 $[M-H]^-$ (upper trace) and calculated exact mass spectrum for compound **8** ($C_{22}H_{29}O_4$) in negative mode.

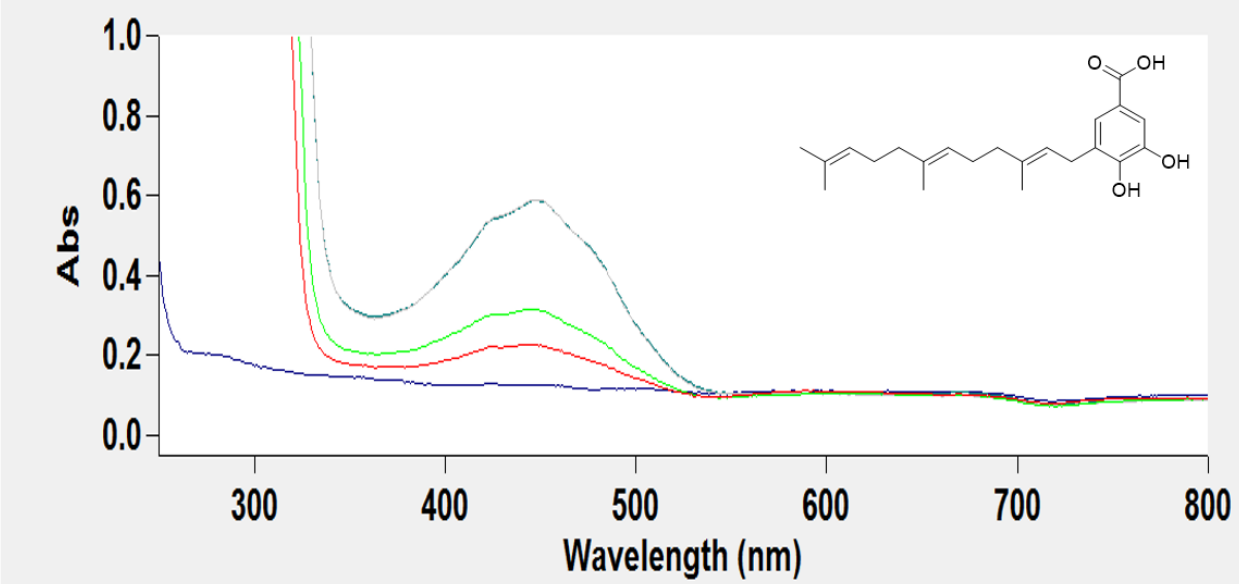

Supplementary Fig. 36. UV-Vis spectra of 3-farnesyl-4,5-dihydroxybenzoic acid (8) in $CDCl_3$.
Blue - $CDCl_3$, green - compound **8** - light green - compound **8** (4x dilution), red - compound **8** (8x dilution). Exact maximum: 447.053 nm, Abs 0.5896.

Supplementary Data Table 1.
X-ray data collection and refinement statistics.

	MstE WT apo	**MstE WT FS-DHB**	**MstE D109A MA**	**MstE D109N GG-DHB**	**MstE Y157F apo**	**MstE R337A GG-DHB**
Crystal parameters						
Space group	P1	$P2_12_12_1$	$P2_12_12_1$	$P2_12_12_1$	$P2_12_12_1$	$P2_12_12_1$
Cell constants	a = 48.5 Å b = 48.6 Å c = 78.0 Å α = 89.0° β = 100.0° γ = 101.9°	a = 48.0 Å b = 77.4 Å c = 90.9 Å	a = 48.0 Å b = 76.8 Å c = 91.3 Å	a = 47.8 Å b = 77.3 Å c = 91.2 Å	a = 47.8 Å b = 77.4 Å c = 91.4 Å	a = 48.0 Å b = 77.8 Å c = 91.6 Å
Subunits/AU[a]	2	1	1	1	1	1
Data collection						
Beam line	X06SA, SLS	X06SA, SLS	X06SA, SLS	X06SA, SLS	X06SA, SLS	X06SA, SLS
Wavelength (Å)	1.0	1.0	1.0	1.0	1.0	1.0
Resolution range (Å)[b]	50-1.95 (2.05-1.95)	50-1.35 (1.45-1.35)	50-1.4 (1.5-1.4)	50-1.4 (1.5-1.4)	50-1.3 (1.4-1.3)	50-2.3 (2.4-2.3)
No. observations	106,013	275,959	342,314	344,128	431,674	79,847
No. unique reflections[c]	46,089[#]	72,004[#]	66,812[#]	66,882[#]	83,943[#]	15,698[#]
Completeness (%)[b]	92.2 (92.5)	95.9 (98.1)	99.4 (99.3)	99.5 (99.6)	99.8 (99.9)	99.3 (99.8)
R_{merge} (%)[b, d]	4.9 (54.9)	4.1 (58.2)	5.3 (50.1)	5.6 (53.7)	4.4 (56.2)	13.7 (57.0)
I/σ (I)[b]	9.4 (2.0)	15.7 (2.6)	16.0 (3.5)	15.4 (3.1)	16.7 (2.7)	9.3 (3.5)
Refinement (REFMAC5)						
Resolution range (Å)	30-1.95	30-1.35	30-1.4	30-1.4	30-1.3	30-2.3
No. refl. working set	43,775	68,352	63,405	63,472	79,680	14,846
No. refl. test set	2,304	3,598	3,337	3,340	4,194	781
No. non-hydrogen	5,608	3,128	3,151	3,228	3,114	2,890
No. ligand		26	31	31		31
Solvent (H_2O, ions)	236	316	338	324	332	91
R_{work}/R_{free} (%)[e]	17.3/20.6	11.5/15.3	10.9/14.8	10.1/13.8	11.5/14.7	18.5/22.9
r.m.s.d. bond (Å)/angle (°)[f]	0.007/1.0	0.014/1.9	0.015/1.8	0.015/1.9	0.015/1.9	0.002/0.94
Average B-factor (Å^2)	12.3	18.3	16.4	17.4	19.3	30.3
Ramachandran Plot (%)[g]	98.1/1.7/0.2	98.3/1.7/0.0	98.3/1.7/0.0	98.3/1.7/0.0	98.2/1.8/0.0	98.6/1.4/0.0
PDB ID	**6SBB**	**6SBC**	**6SBD**	**6SBE**	**6SBF**	**6SBG**

[a] Asymmetric unit

[b] The values in parentheses for resolution range, completeness, R_{merge} and I/σ (I) correspond to the highest resolution shell

[c] Data reduction was carried out with XDS and from a single crystal.
*Friedel pairs were treated as individual reflections
[#]Friedel pairs were treated as identical reflections

[d] $R_{merge}(I) = \Sigma_{hkl}\Sigma_j \mid I(hkl)_j - \langle I(hkl)\rangle \mid / \Sigma_{hkl}\, \Sigma_j\, I(hkl)_j$, where $I(hkl)_j$ is the j^{th} measurement of the intensity of reflection hkl and $\langle I(hkl)\rangle$ is the average intensity

[e] $R = \Sigma_{hkl} \mid \mid F_{obs} \mid - \mid F_{calc} \mid \mid / \Sigma_{hkl} \mid F_{obs} \mid$, where R_{free} is calculated without a sigma cut off for a randomly chosen 5 % of reflections, which were not used for structure refinement, and R_{work} is calculated for the remaining reflections

[f] Deviations from ideal bond lengths/angles

[g] Percentage of residues in favored/allowed/outlier region

Supplementary Table 2.
NMR data for MB (**9**) measured in acetonitrile-d_3.

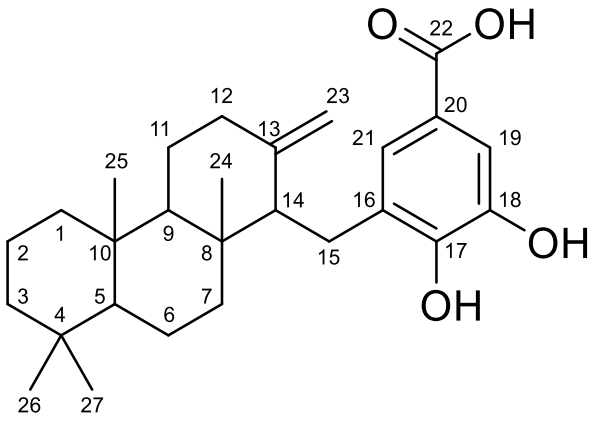

no.	^{1}H	^{13}C	no.	^{1}H	^{13}C
1	0.89 m	40.7	13		149.5
	1.68 m		14	2.28 m	57.0
2	1.64 m	19.4	15	2.74 m	23.7
	1.41 m		16		129.8
3	1.37 m	42.7	17	7.35 brd	124.3
	1.18 m		18		121.4
4		33.9	19	7.24 brd	114.1
5	0.95 m	57.2	20		144.3
6	1.62 m	19.8	21		148.6
	1.45 m		22		167.7
7	1.95 m	41.4	23	4.69 s	107.7
	1.33 m			4.59 s	
8		40.9	24	0.82 s	15.8
9	1.22 m	61.1	25	0.87 s	16.6
10		38.6	26	0.89 s	33.7
11	1.72 m	24.0	27	0.84 s	21.8
	1.35 m				
12	2.32 m	38.8			
	1.94 m				

Supplementary Table 3.
Sitting-drop crystallization parameters of diffracting crystals.

Protein	Conc. [mg/mL]	Protein-reservoir ratio [µL/µL]	Reservoir
MstE apo	15	0.3 + 0.1	0.1 M Tris/HCl, pH 8.5 25% PEG 8000
MstE F-DHB	15	0.2 + 0.2	0.1 M Hepes, pH 7.0 4.0 M NaCl
MstE D109A	15	0.2 + 0.2	0.1 M Hepes, pH 7.0 1.0 M LiCl 30% PEG 6000
MstE D109N	15	0.2 + 0.2	0.1 M Sodium acetate 1.0 M LiCl 30% PEG 6000
MstE Y157F	15	0.2 + 0.1	3.4 M Sodium formate, pH 6.5
MstE R337A	15	0.2 + 0.2	0.5 M LiCl 1.6 M $(NH_4)_2SO_4$

Supplementary Table 4.
Structurally related proteins identified by DALI searches (*35*). The three best hits are shown.

PDB ID	Z-score	R.m.s.d. [Å]	Identity [%]	PDB entry
2SQC	31.1	2.7	21	Squalene-hopene cyclase from *Alicyclobacillus acidocaldarius* (*28*)
5BP8	27.9	2.4	22	Ent-copalyl diphosphate synthase from *Streptomyces platensis* (*16*)
1W6K	27.0	2.7	20	Structure of human OSC in complex with Lanosterol (*15*)

Supplementary Table 5.
Primer sequences used for MstE mutagenesis for crystallization experiments.

MstE mutant	Forward primer (5'-3')	Reverse primer (5'-3')
D109A	GC GGT GAC GCT GCC ACC ACC GGT TG	CA ACC GGT GGT GGC AGC GTC ACC GC
D109N	CTG TGC GGT GAC GCT AAC ACC ACC GGT	ACC GGT GGT GTT AGC GTC ACC GCA CAG
Y157A	T GAA GAA TCT ATC CGT GCT GCC ATC AAA GTT CCG GAC CTG	CAG GTC CGG AAC TTT GAT GGC AGC ACG GAT AGA TTC TTC A
Y157F	A GAA TCT ATC CGT GCT TTC ATC AAA GTT CCG GAC C	G GTC CGG AAC TTT GAT GAA AGC ACG GAT AGA TTC T
R337A	C TAC GAC GAA ATC GAA GGT GAC AAA GCT TTC GAA GGT TCT A	T AGA ACC TTC GAA AGC TTT GTC ACC TTC GAT TTC GTC GTA G
R339Q	C GAA GGT GAC AAA CGT TTC CAG GGT TCT ATC ATC TTC GAC C	G GTC GAA GAT GAT AGA ACC CTG GAA ACG TTT GTC ACC TTC G

Supplementary Table 6.

Primers used for introducing single point mutations for activity screening.

MstE mutant	Forward primer (5'-3')	Reverse primer (5'-3')
F49A	G TGG TGG CAG GAC TTC AAT GCC CCT CAG GCT GCT AGC ATC	GAT GCT AGC AGC CTG AGG GGC ATT GAA GTC CTG CCA CCA C
W59A	C ATC GGT GAT GAG GCG GTG ACG GCT TAT G	C ATA AGC CGT CAC CGC CTC ATC ACC GAT G
Y100A	CA GGT GAG TGG GGT GCT AAC TAC ATT CTC TG	CA GAG AAT GTA GTT AGC ACC CCA CTC ACC TG
D109S	C ATT CTC TGT GGA GAT GCG TCC ACT ACG GGC TGG GCA TTA C	G TAA TGC CCA GCC CGT AGT GGA CGC ATC TCC ACA GAG AAT G
F149A	C AAT GGT GGG ATA GCG ACC GCC GCT GAG GAA TCG ATT CG	CG AAT CGA TTC CTC AGC GGC GGT CGC TAT CCC ACC ATT G
F149Y	GG ATA GCG ACC TAC GCT GAG GAA TCG	CGA TTC CTC AGC GTA GGT CGC TAT CC
F149W	GT GGG ATA GCG ACC TGG GCT GAG GAA TCG ATT C	G AAT CGA TTC CTC AGC CCA GGT CGC TAT CCC AC
Y157A	GAA TCG ATT CGA GCC GCT ATT AAG GTT CCC G	C GGG AAC CTT AAT AGC GGC TCG AAT CGA TTC
W171F	C TCG TTT CAG GGT TTC TGC GGA GCC CAT AC	GT ATG GGC TCC GCA GAA ACC CTG AAA CGA G
W210A	GGG AAC TGG GAA GGT TAT GCG TGG AGT GAT CAT GAA TAC	GTA TTC ATG ATC ACT CCA CGC ATA ACC TTC CCA GTT CCC
Y216F	GG AGT GAT CAT GAA TTC ACC ACG GCA TTA AC	GT TAA TGC CGT GGT GAA TTC ATG ATC ACT CC
I312F	CA TCT GCT TAC CTG CGG TTT CCC TAT CCT TTT GAT CG	CG ATC AAA AGG ATA GGG AAA CCG CAG GTA AGC AGA TG
F338A	G ATT GAA GGA GAC AAG AGG GCT GAA GGA AGT ATT ATT TTC	GAA AAT AAT ACT TCC TTC AGC CCT CTT GTC TCC TTC AAT C
F350Y	GAT CAC AAC AGC ATT TAC ACC ACT GCT ACT GTC	GAC AGT AGC AGT GGT GTA AAT GCT GTT GTG ATC